ABSTRACT

DALEO, NOAH S. Algorithms and Applications in Numerical Elimination Theory. (Under the direction of Jonathan D. Hauenstein.)

Numerical algebraic geometry provides tools for solving systems of polynomial equations and manipulating their solution sets. The focus of this dissertation is the application of these tools to problems arising in elimination theory. In Chapter 1, we introduce numerical elimination theory and provide motivation for the methods that follow. In Chapter 2, we provide prerequisite background material from classical and numerical algebraic geometry. In Chapter 3, we establish an effective numerical test for determining whether or not a polynomial image of an algebraic set is arithmetically Cohen-Macaulay. Using the results of this test, we compute several properties describing the structure of the image. In Chapter 4, we focus on discriminant loci, which arise as elimination problems when one wants to compute special points in a parameter space. Finally, in Chapter 5, we focus on the special case in which a polynomial image of an algebraic set is a secant variety. As we introduce new algorithms throughout this work, we demonstrate their effectiveness on examples and applications. These applications include an investigation of the vacuum space in the Minimal Supersymmetric Standard Model, computing the critical coupling strength for synchronization in the Kuramoto model, and testing the validity of a model in lattice field theory.

Algorithms and Applications in Numerical Elimination Theory

by
Noah S. Daleo

A dissertation submitted to the Graduate Faculty of
North Carolina State University
in partial fulfillment of the
requirements for the Degree of
Doctor of Philosophy

Mathematics

Raleigh, North Carolina

2015

APPROVED BY:

Daniel J. Bates	Radmila Sazdanović
Seth Sullivant	Agnes Szanto

Jonathan D. Hauenstein
Chair of Advisory Committee

DEDICATION

To my wife, Rhonda.

BIOGRAPHY

Noah Daleo was born in Freehold, NJ and spent his childhood in Jackson, NJ, where he attended Jackson Memorial High School. During his teenage years, he developed an interest in science and math. An interest in astronomy led him to pursue a physics major, which he eventually switched to math. Noah graduated with a B.S. in Mathematics from Kennesaw State University in 2010. He spent the next five years at North Carolina State University studying and teaching math. During this time, he completed a M.S. in Mathematics and became interested in numerical algebraic geometry. At the time of this writing, he is planning to move to Massachusetts and is looking forward to a career in academia.

ACKNOWLEDGEMENTS

I would like to begin by thanking my advisor Jonathan Hauenstein for his guidance and dedication over the past few years. I am tremendously grateful for the opportunity to have worked with him. To put it simply, I could not have asked for a better advisor.

I thank my committee members Dan Bates, Radmila Sazdanović, Seth Sullivant, and Agnes Szanto for helpful discussions and for providing me with motivation.

During the past few years, I have been fortunate to work with a number of other people. I thank my collaborators Alessandra Bernardi, Daniel Brake, Florian Dörfler, Yang-Hui He, Dhagash Mehta, Bernard Mourrain, Brent Nelson, Luke Oeding, and Christopher Seaton.

I owe great thanks to my undergraduate advisor at Kennesaw State University, Ana-Maria Croicu. Her advice and encouragement came at a crucial time in my academic development and led me to where I am today.

Finally, none of this would have been possible without the love and support of my wife, Rhonda. She is my constant source of inspiration and strength. Rhonda was by my side when I returned to college, completed my B.S., applied to graduate school, studied for qualifying exams, and began teaching. She has been the first to hear of my struggles and successes during the research for this dissertation. I cannot thank her enough.

TABLE OF CONTENTS

LIST OF TABLES

LIST OF FIGURES

Chapter 1

Introduction

1.1 An illustrative example

A classical object in algebraic geometry is the *twisted cubic curve*, which can be written as

$$X = \left\{(x, y, z) \in \mathbb{C}^3 \ : \ F(x, y, z) = 0\right\} \text{ where } F(x, y, z) = \begin{bmatrix} y - x^2 \\ z - x^3 \end{bmatrix} \tag{1.1}$$

or as

$$X = \overline{\pi(\mathbb{C})} \text{ where } \pi : \mathbb{C} \to \mathbb{C}^3 \text{ is given by } \pi(t) = (t, t^2, t^3), \tag{1.2}$$

where the closure is in the standard complex topology. We say that (1.1) is an *implicitization* of X and (1.2) is a *parameterization* of X.

Both of these constructions are useful in different ways. From (1.1), we can quickly see that the points in X describe the intersection of two surfaces in $\mathbb{C}^3$. Specifically, the set of points (x, y, z) satisfying $y - x^2 = 0$ forms a surface, and the set of points (x, y, z)

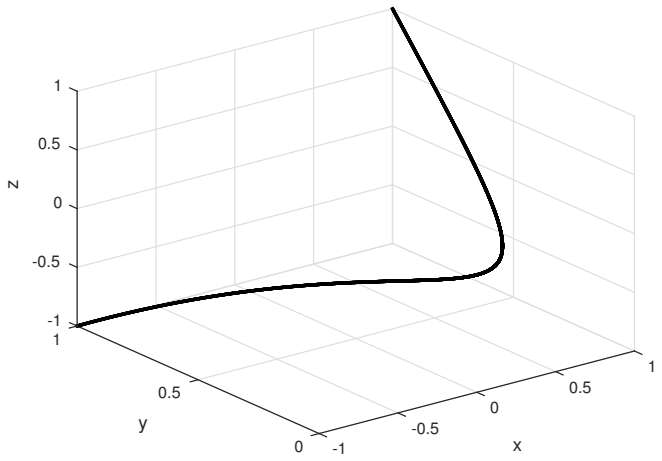

Figure 1.1: The twisted cubic curve X.

satisfying $z - x^3 = 0$ forms a surface; we see that X is the intersection of these two sets. On the other hand, from (1.2), we can quickly see that every point on $\mathbb{C}$ maps to a point on X. In this way, our two characterizations of X highlight different features of the set.

A natural question is the following:

Given a parameterization, can we compute an implicitization?

For the twisted cubic curve, we may start with (1.2) and write

$$\begin{aligned} X &= \overline{\pi(\mathbb{C})} \text{ where } \pi : \mathbb{C} \to \mathbb{C}^3 \text{ is given by } \pi(t) = (t, t^2, t^3) \\ &= \{(x, y, z) \ : \ x = t, \ y = t^2, \ z = t^3\}. \end{aligned}$$

We then *eliminate* t from the system:

$$\begin{bmatrix} x - t \\ y - t^2 \\ z - t^3 \end{bmatrix} = 0 \quad \longrightarrow \quad F(x, y, z) = \begin{bmatrix} y - x^2 \\ z - x^3 \end{bmatrix}.$$

Thus, elimination of variables is an important goal if we want to translate from one construction to the other. Since an implicitization indicates certain structure of the set, this elimination problem is an important one. If our equations were linear rather than polynomial, then we could eliminate variables using Gaussian elimination. Instead, we must use other methods.

1.2 Symbolic elimination theory

For the elimination problem posed in Section 1.1, the equation $x = t$ made it easy for us to eliminate t. Here, we consider an example in which a more sophisticated method is preferred.

Let $\pi : \mathbb{C}^2 \to \mathbb{C}^2$ be the map $\pi(x, y) = (x^2, y^3)$, and let

$$A = \left\{(x, y) \in \mathbb{C}^2 \ : \ x^2 + y^2 - 1 = 0\right\} \text{ and } X = \overline{\pi(A)}.$$

Although $A \subset \mathbb{C}^2$ and $X \subset \mathbb{C}^2$, we can plot points in $\mathbb{R}^2$ to gain some intuition of the problem. Figure 1.2 depicts the real-valued points of A and X.

Note that we have an implicitization for A, but we only have a parameterization of X. This will be a common theme. To find an implicitization for X, we want to eliminate x and y from a system of polynomial equations. Our problem is of the form:

$$\begin{bmatrix} z_1 - x^2 \\ z_2 - y^3 \\ x^2 + y^2 - 1 \end{bmatrix} = 0 \qquad \longrightarrow \qquad F(z_1, z_2) = ?$$

One method for solving problems of this form utilizes the multivariate resultant,

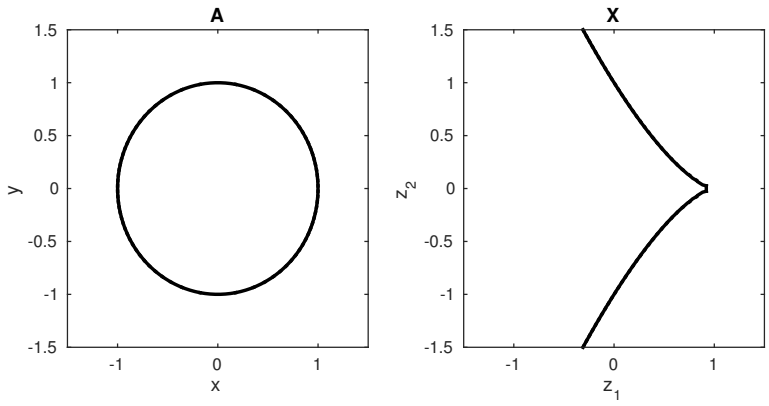

Figure 1.2: Real-valued points of A and $X = \overline{\pi(A)}$.

introduced by Macaulay in 1902 [Mac02]. At roughly the same time, Gordan introduced what would eventually become known as Gröbner bases, but he did not have an algorithm for computing one at the time [Gor99]. It was Buchberger's 1965 Ph.D. thesis [Buc65] that introduced such an algorithm. The resultant and Gröbner basis methods are powerful tools for eliminating variables from systems of polynomials. For our problem above, Buchberger's algorithm computes a set of polynomials $\mathcal{A} = \{f_1, \ldots, f_r\}$ such that the polynomial we seek is

$$F = \begin{bmatrix} f_{\alpha_1} \\ \vdots \\ f_{\alpha_s} \end{bmatrix}$$

where $f_{\alpha_1}, \ldots, f_{\alpha_s}$ are precisely the elements of $\mathcal{A}$ that are polynomials in x, y [Has06]. Modern software implementations based on these methods include Maple 16 [Map12] and Macaulay2 [GS]. Using Maple's `EliminationIdeal` command, we find

$$X = \left\{(z_1, z_2) \in \mathbb{C}^2 \ : \ F(z_1, z_2) = 0\right\} \text{ where } F(z_1, z_2) = z_1^3 - 3z_1^2 + z_2^2 + 3z_1 - 1.$$

This polynomial F was used earlier when plotting X in Figure 1.2.

In addition to Buchberger's algorithm, more recent algorithms have been developed for computing Gröbner bases, including strategies utilizing numerical methods (e.g., [Kon04]) and parallel processing (e.g., [Amr96]). In particular, [Fau99] uses sparse linear algebra methods to facilitate simultaneous reduction of several polynomials instead of the traditional polynomial reduction found in Buchberger's algorithm. A more recent method [Fau02] detects superfluous critical pairs to reduce the amount of time spent on S-polynomials that reduce to zero. An overview of some recent developments can be found in [EF14].

1.3 Numerical elimination theory

In practice, elimination problems may arise that are difficult or impractical to solve symbolically. For example, in Section 3.5.2 we will define polynomial systems $G : \mathbb{C}^{16} \to \mathbb{C}^{16}$ and $\pi : \mathbb{C}^{16} \to \mathbb{C}^{25}$. As we will see, a problem arising in theoretical physics is the study of the set

$$X = \overline{\pi(V)} \text{ where } V = \{x \in \mathbb{C}^{16} \ : \ G(x) = 0\}. \tag{1.3}$$

Although an implicitization of X exists, an attempt at computing one using Macaulay2 was unsuccessful after running for 4 weeks. Problems such as these motivate us to develop new strategies for studying X, whether by computing an implicitization or through other methods.

In 1996, Sommese and Wampler coined the term *numerical algebraic geometry* (NAG) to describe a new research area focused on the numerical solution of systems of polynomial equations [Som96]. Simply put, NAG is to algebraic geometry what numerical linear

algebra is to linear algebra. Recent developments in this area provide a new set of tools to apply to elimination problems. Using information from the fiber set V, we may be able to perform operations on the image X [HS10]. For example, this allows one to test points for membership in an image [HS13]. Applications of numerical elimination theory include the moduli space of vacua [Hau13b], the computational complexity of matrix multiplication [Hau13a], tensor decomposition [Hau14], and computing algebraic matroids [Ros14].

The goal of this work is to make advances in the numerical study of sets arising in elimination problems. In some cases this may lead to computing the corresponding polynomial system as we did in Sections 1.1 and 1.2. However, in most cases, such as the set X in (1.3), we will forgo the determination of polynomials and instead study the set geometrically. In doing so, we will avoid difficult Gröbner basis and resultant computations.

Chapter 2

Background

2.1 Preliminaries from algebraic geometry

Let $\mathbb{C}$ denote the field of complex numbers and let $\mathbb{C}[x_1, \ldots, x_n]$ denote the ring of polynomials in $x_1, \ldots, x_n$ with coefficients in $\mathbb{C}$. We may write a polynomial $f \in \mathbb{C}[x_1, \ldots, x_n]$ in *multi-index notation* as

$$f = \sum_{\alpha \in \mathcal{A}} c_\alpha x^\alpha,$$

where $\mathcal{A}$ is a finite set of n-tuples of nonnegative integers, $c_\alpha = c_{\alpha_1 \ldots \alpha_n}$, $x^\alpha = x_1^{\alpha_1} \ldots x_n^{\alpha_n}$, and $|\alpha| = \sum_{i=1}^n \alpha_i$. The *degree* of f is $\deg f = \{\max |\alpha| \ : \ \alpha \in \mathcal{A}, c_\alpha \neq 0\}$. If $c_\alpha = 0$ whenever $|\alpha| < \deg f$, then f is said to be *homogeneous*.

We will often work with a system $F = \begin{bmatrix} f_1 \\ \vdots \\ f_m \end{bmatrix}$ such that $f_1, \ldots, f_m \in \mathbb{C}[x_1, \ldots, x_n]$. Given such a system F, we define the *algebraic set*

$$V(F) = \{x \in \mathbb{C}^n \ : \ F(x) = 0\},$$

where 0 is understood to represent the n-vector of all zeros. The system F is said to *define* the algebraic set $V(F)$. In Section 2.3, we will see that an algebraic set is either reducible or irreducible. Some authors refer to any algebraic set $V(F)$ as a *variety*, but other authors only use this term to refer to an irreducible algebraic set. To avoid this ambiguity, we will typically avoid the term variety. We define the *ideal generated by* F as

$$I(F) = \left\{ \sum_{1}^{m} h_i f_i \ : \ h_1, \ldots, h_m \in \mathbb{C}[x_1, \ldots, x_n] \right\}.$$

Algebraic sets and ideals are fundamental objects for working with sets of polynomials geometrically and algebraically, respectively. Every algebraic set $X \subseteq \mathbb{C}^n$ has a corresponding system of polynomials F, but we may investigate X geometrically without explicitly knowing F. Similarly, from Hilbert's Basis Theorem, we know that every ideal in $\mathbb{C}[x_1, \ldots, x_n]$ is generated by a finite number of polynomials, but we may discuss an ideal I whose defining equations F are not known.

In some cases, we may wish to work in *n-dimensional projective space*, which is denoted $\mathbb{P}^n$ and defined as follows. Consider the equivalence relation $\sim$ on the nonzero points of $\mathbb{C}^{n+1}$ such that $x \sim y$ if and only if there is a nonzero element $\lambda \in \mathbb{C}$ such that $x = \lambda y$. Then we define $\mathbb{P}^n = (\mathbb{C}^{n+1} - \{0\}) / \sim$. In projective space we work with homogeneous polynomials, because these satisfy the property $f(\lambda x) = \lambda^{\deg f} f(x)$. If $g \in \mathbb{C}[x_1, \ldots, x_n]$ is not homogeneous, then we can always construct a corresponding homogeneous polynomial in $\mathbb{C}[x_0, x_1, \ldots, x_n]$ by multiplying each monomial of g with the appropriate power of x_0. We refer to $V(F) \subseteq \mathbb{P}^n$ as a *projective algebraic set*. When the context is clear, we will refer to both $V(G) \subseteq \mathbb{C}^n$ and $V(F) \subseteq \mathbb{P}^n$ simply as algebraic sets.

2.2 The general form of problems

In this section, we formalize the type of problem introduced in Chapter 1. Given two known polynomial maps

$$G : \mathbb{C}^m \to \mathbb{C}^k \text{ and } \pi : \mathbb{C}^m \to \mathbb{C}^n,$$

our object of interest is

$$X = \overline{\pi(V(G))} \subset \mathbb{C}^n,$$

where the closure is in the usual complex topology. From the following theorem, we know that $\pi(V(G))$ is a *constructible set*, meaning that it is constructed by starting with algebraic sets and performing a finite sequence of the operations of union, intersection, and complementation.

Theorem 2.2.1 (Chevalley's Theorem [Bat13]) *Let $f : A \to B$ be an algebraic map between algebraic sets and let $Z \subset A$ be constructible. Then $f(Z)$ is a constructible set.*

We make use of the following lemma.

Lemma 2.2.2 (Lemma 16.2 of [Bat13]) *Let $W \subset \mathbb{C}^N$ be a constructible set. Then the closure $\overline{W}$ of W in the usual topology is an algebraic set.*

Thus, $X = \overline{\pi(V(G))}$ is an algebraic set. In other words, the expression $\overline{\pi(V(G))}$ has the same meaning whether we consider the closure to be in the usual topology or the Zariski topology on $\mathbb{C}^n$.

Another way to view X is to consider

$$H(x,y) = \begin{bmatrix} y - \pi(x) \\ G(x) \end{bmatrix}$$

where $x = (x_1, \ldots, x_m)$ and $y = (y_1, \ldots, y_n)$. If we define the projection map $\gamma : \mathbb{C}^{m+n} \to \mathbb{C}^n$ so that $\gamma(x,y) = y$, then we have

$$X = \overline{\gamma(V(H))}. \tag{2.1}$$

Thus, we want to eliminate the fiber variables x to acquire a set only in the image coordinates y. Algebraically, $X = V(J)$ where J is the *elimination ideal* $J = I(H) \cap \mathbb{C}[y]$. The primary goal of classical elimination theory is to symbolically compute the generators of J, because they describe and *define* X. In numerical elimination theory, our goals include computing properties describing X and J, locating points of interest in X, and testing points for membership in X.

2.3 Irreducible decomposition

2.3.1 Reducible and irreducible algebraic sets

An algebraic set X is said to be *reducible* if there exist algebraic sets X_1, X_2 such that $X = X_1 \cup X_2$ with $X \neq X_1$ and $X \neq X_2$. If X is not reducible, then it is said to be *irreducible*. Irreducible algebraic sets can be thought of as the building blocks of all algebraic sets in the following sense.

Theorem 2.3.1 (e.g., Theorem 4 of [Cox07]) *Let $X \in \mathbb{C}^n$ be an algebraic set. Then*

there exists a unique decomposition

$$X = X_1 \cup \cdots \cup X_k$$

such that each X_i is an irreducible algebraic set and $X_i \not\subset X_j$ for all $i \neq j$. This decomposition is unique up to reordering.

2.3.2 Dimension, degree, and multiplicity

Let $X \subset \mathbb{C}^n$ be an algebraic set. A point $p^* \in X$ is called a *manifold point of X* if it has a neighborhood $U \subset X$ for which there exists a mapping ϕ sending U one-to-one and onto a neighborhood of the origin in $\mathbb{C}^k$. The integer k is called the *local dimension* of X at p^*, which we denote $\dim_{p^*} X$. The set of manifold points of X is dense in X [Bat13]. For an arbitrary point $x^* \in X$, we define $\dim_{x^*} X$ to be the maximum local dimension of the irreducible components containing x^*. Finally, we define the *dimension* of X as

$$\dim X = \max\{\dim_{x^*} X \ : \ x^* \in X\}.$$

If all of the irreducible components of X are the same dimension, then we say X is *pure-dimensional*.

With respect to polynomials, we are used to the notion that 0 has multiplicity 1 with respect to $f(x) = x$ and multiplicity 2 with respect to $f(x) = x^2$. However, with respect to algebraic sets, we note that $V(x) = V(x^2)$. Therefore, multiplicity is a piece of information missing from algebraic sets. However, given $X = V(f)$, we may consider the corresponding scheme $f^{-1}(0)$, which contains points as well as multiplicity information. We say that the *multiplicity of X with respect to f* is the multiplicity of a smooth point

of X when considered as a solution to $f(x) = 0$.

As we will see, a common construction in numerical algebraic geometry is the intersection of an algebraic set with a generic linear space of carefully chosen dimension. We may refer to this process as *slicing* or *taking linear sections*. Let $X \subset \mathbb{C}^n$ be an algebraic set of dimension d, and let L be a generic linear space of codimension d. That is, $L = V(P)$ where $P : \mathbb{C}^n \to \mathbb{C}^d$ is a generic linear map; in practice, we may define P by a randomly generated matrix. Then the intersection $X \cap L$ consists of a finite number of points, and we define the *degree* of X as $\deg X = |X \cap L|$. This leads us to the notion of a witness set.

2.4 Numerical algebraic geometry

2.4.1 Witness sets and sampling

The fundamental data structure for representing an irreducible algebraic set in numerical algebraic geometry, a *witness set*, is based on linear sections of complimentary dimension. Let $F \in \mathbb{C}[x_1, \ldots, x_n]$ be a system of polynomials and let $V \subset \mathbb{P}^n$ be an irreducible algebraic set of dimension d which is an irreducible component of $V(F)$. Then, a *witness set* for V is a triple $\{F, L, W\}$ where $L \subset \mathbb{P}^n$ is a general linear space of codimension d and $W = V \cap L \subset \mathbb{P}^n$ is a *witness point set* consisting of $\deg V$ points. We refer the reader to [SW05] for more details about witness sets.

Example 2.4.1 *Consider the following curve in* $\mathbb{P}^3$*:*

$$C = \{(s^3, s^2t, st^2, t^3) \ : \ (s, t) \in \mathbb{P}^1\},$$

which is the algebraic set defined by

$$F(w,x,y,z) = \begin{bmatrix} xz - y^2 \\ yw - z^2 \\ xw - yz \end{bmatrix} = 0.$$

This is the projectivization of the twisted cubic curve discussed in Section 1.1; note that we can recover the formulation of (1.1) by setting $w = 1$ *and simplifying. To construct a witness set for* C*, consider* $L = V(\sqrt{2}w + \sqrt{-3}x + \sqrt{5}y + \sqrt{-7}z)$*. Then a witness set for* C *is* $\{F, L, W\}$ *where* $W := C \cap L$ *consists of the* 3 *points*

$$\begin{aligned} W = \{&(0.152026i, 1, -0.533711i, -0.284847), \\ &(1, -0.079630i, -0.185091, 0.430222i), \\ &(-0.962272i, 1, -0.987262i, -0.974687)\}. \end{aligned}$$

We note that L *was chosen here for readability and the points of* W *have been rounded to* 6 *digits. In typical use, a generic linear space* L *would be used.*

One key operation in numerical algebraic geometry, called *sampling*, is the ability to use a witness set $\{f, L, W\}$ for an algebraic set V to produce a collection of arbitrarily close numerical approximations of arbitrarily many smooth points on V. In particular, suppose that $x \in W = V \cap L$ and let $L^* \subset \mathbb{P}^n$ be a linear space of codimension d. Consider the path $z(t) : [0,1] \to V$ defined by $z(1) = x$ and $z(t) \in V \cap (t \cdot L + (1-t) \cdot L^*)$. Except on a Zariski closed proper subset of choices for L^*, $z(t)$ is a smooth point of V for all $t \in [0,1]$, i.e., $z(0)$ is also a smooth point of V. We note the smooth points of V are (path) connected since V is irreducible. Linear sections and witness sets are also used

in membership testing; more details regarding these algorithms can be found in [Som01; SW05].

Suppose we are given a problem of the form introduced in Section 2.2 in which we wish to study irreducible components of $X = \overline{\pi(V(G))} \subset \mathbb{C}^n$ for polynomial systems $G : \mathbb{C}^m \to \mathbb{C}^k$ and $\pi : \mathbb{C}^m \to \mathbb{C}^n$. In this case, the defining equations for X may not be readily available; indeed, determining them is the primary goal of classical elimination theory. Since the construction of a witness set requires defining equations, we instead utilize an analogous data structure known as a *pseudowitness set* [HS10; HS13]. First, let $H : \mathbb{C}^{m+n} \to \mathbb{C}^{k+n}$ and $\gamma : \mathbb{C}^{m+n} \to \mathbb{C}^n$ be the maps defined in (2.1) so that $X = \overline{\gamma(V(H))}$. Let $V \subset V(H) \subset \mathbb{C}^{m+n}$ be an irreducible algebraic set so that $Y := \overline{\gamma(V)} \subset X$ is irreducible. Let $d = \dim V$ and $\ell = \dim Y$, which we will show how to compute in Section 2.4.2. A pseudowitness set for Y is a set $\{H, \gamma, \mathcal{L}, W\}$ where $\mathcal{L} \subset \mathbb{C}^{m+n}$ is the linear space constructed as follows and $W = V \cap \mathcal{L} \subset \mathbb{C}^{m+n}$. Let $L_1 : \mathbb{C}^{m+n} \to \mathbb{C}^\ell$ be the map defined by $L_1(x, y) = L(\gamma(x, y))$ where $L : \mathbb{C}^n \to \mathbb{C}^\ell$ is a general linear system, and let $L_2 : \mathbb{C}^{m+n} \to \mathbb{C}^{d-\ell}$ be a general linear system. Then we construct $\mathcal{L} = V(L_1, L_2) \subset \mathbb{C}^{m+n}$. With this setup, W is a finite set and we have $|\gamma(W)| = \deg Y$.

2.4.2 Computing a pseudowitness set

Let $G : \mathbb{C}^m \to \mathbb{C}^k$ and $\pi : \mathbb{C}^m \to \mathbb{C}^n$ be known polynomial maps. We have seen in (2.1) that an irreducible component $Y \subset \overline{\pi(V(G))}$ can be written as an image of a linear projection γ. Our present goal is to compute a pseudowitness set $\{H, \gamma, \mathcal{L}, W\}$ for Y as defined in 2.4.1. The construction of H, γ, and $\mathcal{L}$ are straightforward, and this section will describe how to compute the *pseudowitness point set* W from G and π. Although an algorithm can be found in [HS10], in this section we describe an algorithm that relies on

monodromy loops.

We assume that we already have a witness set for V, which can be computed via a standard procedure in numerical algebraic geometry, e.g., as implemented in `Bertini` [Bat]. We also assume that we know $\dim Y$, which can be determined as follows. First, if the multiplicity of V is greater than 1, then we use isosingular deflation [HW13] to reduce to a multiplicity 1 case. Let z^* be a generic point on V. Then with probability one by Lemma 3 of [HS10],

$$\dim Y = \dim V - \dim \text{ null} \begin{bmatrix} J\pi(z^*) \\ JG(z^*) \end{bmatrix}$$

where $\dim V$ is already known from the witness set for V.

Let $d = \dim V$ and $\ell = \dim Y$. Let v^* be a sufficiently general point in V, which in practice is accomplished by choosing a witness point. Let $y^* = \pi(v^*) \in Y$. Construct general linear systems $L : \mathbb{C}^n \to \mathbb{C}^\ell$ and $L' : \mathbb{C}^m \to \mathbb{C}^{d-\ell}$ such that $L(y^*) = 0$ and $L'(v^*) = 0$.

We will use monodromy loops to compute the pseudowitness point set W. First, set $W := \{v^*\}$. Each monodromy loop will be performed using two homotopies as follows. Choose random vectors $q^* \in \mathbb{C}^\ell$ and $r^* \in \mathbb{C}^{d-\ell}$, and let the point(s) in W be the start points for the homotopy

$$\begin{bmatrix} G(x) \\ y - \pi(x) \\ L(y) + (1-t)q^* \\ L'(x) + (1-t)r^* \end{bmatrix} = 0$$

as $t \in \mathbb{R}$ continuously deforms from 1 to 0. The endpoints of this homotopy will be used as the start points of the next homotopy.

Let $\alpha \in \mathbb{C}$ be a random constant. We perform the homotopy

$$\begin{bmatrix} G(x) \\ y - \pi(x) \\ L(y) + \frac{\alpha t}{1-t+\alpha t} \cdot q^* \\ L'(x) + \frac{\alpha t}{1-t+\alpha t} \cdot r^* \end{bmatrix} = 0$$

as $t \in \mathbb{R}$ continuously deforms from 1 to 0. Next, we update W to include all distinct endpoints of this homotopy.

The pair of homotopies above comprises one monodromy loop. We repeat these loops using different random vectors q^* and r^* until no new pseudowitness points are found for several loops.

When W is unchanged for several iterations, our next goal is to use a *trace test* to verify that a complete pseudowitness set has been found, i.e., that $|\pi(W)| = \deg Y$. We accomplish this with two more homotopies. Choose random vectors $q^* \in \mathbb{C}^\ell$ and $r^* \in \mathbb{C}^{d-\ell}$. Let

$$H_1(x,y,t) = \begin{bmatrix} G(x) \\ y - \pi(x) \\ L(y) + (1-t)q^* \\ L'(x) + (1-t)r^* \end{bmatrix} = 0 \quad \text{and} \quad H_2(x,y,t) = \begin{bmatrix} G(x) \\ y - \pi(x) \\ L(y) - (1-t)q^* \\ L'(x) - (1-t)r^* \end{bmatrix} = 0.$$

We use the points in W as start points for both homotopies and track solution paths to $H_1 = 0$ and $H_2 = 0$ as t continuously deforms from 1 to 0. Let E_1 and E_2 denote the endpoints of these homotopies, respectively.

We now consider the sets of points $\pi(W)$, $\pi(E_1)$, and $\pi(E_2)$. Since H_1 and H_2 move the

linear space parallel to itself, we can reach a conclusion based on how the pseudowitness points moved. Given corresponding points $w \in \pi(W)$, $e_1 \in \pi(E_1)$, and $e_2 \in \pi(E_2)$, we want to check whether or not $\frac{e_1+e_2}{2} = w$. For each coordinate, we check $\sum(\frac{e_1+e_2}{2} - w)$ where the summation is over all points. If this sum is zero for all coordinates, then $\pi(W)$ describes a linear slice of Y and we have found a pseudowitness set. Otherwise, there are still remaining points to be found for W and we perform more monodromy loops until the trace test is successful.

2.4.3 Homotopy continuation

The key algorithm behind numerical algebraic geometry is homotopy continuation. A full description of the methods and challenges present in homotopy continuation is outside the scope of this work, but we give an overview below. The interested reader is encouraged to see [SW05; Bat13] for more information.

Let $x = (x_1, \ldots, x_n)$ and suppose we are given a system of polynomial equations,

$$F(x) = \begin{bmatrix} f_1(x) \\ \vdots \\ f_n(x) \end{bmatrix} = 0,$$

for which we want to compute all isolated solutions. We begin by constructing a simpler *start system*,

$$G(x) = \begin{bmatrix} g_1(x) \\ \vdots \\ g_n(x) \end{bmatrix} = 0,$$

whose isolated solutions are known. There are several ways to construct a start system,

with the key requirement being that the number of isolated solutions is an upper bound on the number of isolated solutions for F. For example, one may construct G so that its number of isolated solutions is the Bézout bound, which is $\prod_{i=1}^{n} d_i$ where d_i is the degree of f_i. One way to accomplish this is with the start system $G = (g_1, \ldots, g_n) = 0$ where $g_i(x) = x_i^{d_i} - 1$ for each i.

Next, we consider the homotopy

$$H(x,t) = (1-t)F(x) + \gamma t G(x) = 0,$$

where γ is a general complex number. In this setting, we know the solutions of $H = 0$ when $t = 1$, and we want to compute the solutions of $H = 0$ when $t = 0$. Homotopy continuation entails numerically tracking solution paths via a predictor-corrector method as $t \in \mathbb{R}$ continuously deforms from 1 to 0. In this dissertation, we use the software implementation in `Bertini` [Bat], which uses adaptive precision to track paths within a user-defined tolerance. Since each path can be tracked independently, we make use of parallel processing in these computations.

2.4.4 Parameter homotopies

In some applications, it is useful to study solution sets corresponding to many points in the parameter space. Although this can be accomplished through repeated uses of homotopy continuation, it is inefficient to start over each time. In these situations, we use a two-phase technique known as a *parameter homotopy*. We give a brief overview here, and the reader is directed to [SW05; Bat13] for more details. For simplicity we describe the method for one parameter $P \in \mathbb{C}$, but it is straightforward to generalize this approach to an arbitrary number of parameters.

First, in the ab initio phase, we choose a generic complex parameter $P = P_0 \in \mathbb{C}$ and numerically compute the set of solutions S_0 to the system using homotopy continuation implemented in `Bertini`. Although solving the system for a general value of P is relatively costly, we only perform this computation once, and our subsequent computations make use of these results to significantly reduce the overall effort.

Next, in the parameter homotopy phase, we consider various choices of $P \in \mathbb{C}$. For each value of interest, we use `Bertini` to numerically track solution paths starting at the points in S_0. These paths are defined by a continuous deformation from P_0 to P so that the endpoints are the solutions we want. Each of these computations is relatively inexpensive, thereby making it practical to compute the solutions at hundreds of different choices for P. In particular, we will make use of this technique in Chapter 4 when studying discriminant loci.

Chapter 3

Computing properties with numerical elimination theory

3.1 Introduction

Let $X \subset \mathbb{P}^n$ be a pure-dimensional algebraic set of dimension $d > 0$ arising as a polynomial image of an algebraic set. In this chapter, we introduce strategies for computing properties of X without requiring the defining ideal $I(X)$. A key aspect of this work is determining whether or not X is arithmetically Cohen-Macaulay (aCM), which we define in 3.2.1. We propose a test for deciding if X is aCM given the ability to sample points lying (approximately) on a general curve section of X. This chapter is largely based on [DH15].

An important fact regarding algebraic sets of dimension at least 2 is that arithmetically Cohen-Macaulayness is preserved under slicing by a general hyperplane (or hypersurface). In particular, a pure-dimensional algebraic set X of positive dimension is aCM if and only if a general curve section of X is aCM. In the case that X is a curve, i.e., $\dim X = 1$, a numerical test provided in [Hau09] can determine if X is aCM. This test relies upon

computing Hilbert functions of zero-dimensional schemes defined by intersecting X with general hypersurfaces of various degrees. Unfortunately, due to the increasingly higher degree zero-dimensional schemes under consideration, this test becomes impractical for curves of even moderate degree. Section 3.6.2 presents an example that compares the approach of [Hau09] with our approach.

If X is arithmetically Cohen-Macaulay (aCM) or if $\dim X = 1$, then one of the properties we can compute is the Castelnuovo-Mumford regularity of X. Since we are working over a field of characteristic zero, the Castelnuovo-Mumford regularity is equal to the maximum degree of the elements in a Gröbner basis for $I(X)$ when working with generic coordinates in the reverse lexicographic ordering (see [BS87] for more information). Thus, the Castelnuovo-Mumford regularity provides a measure of complexity for performing symbolic computations on $I(X)$.

The arithmetic and geometric genus are two invariants of a curve C of particular interest in computational algebraic geometry. These genera must be equal if C is smooth. A numerical algebraic geometric procedure for computing the geometric genus is presented in [Bat11] which was extended in [HS13] to curves which arise as the image of an algebraic set under a polynomial map. The geometric genus of a general four-bar coupler curve was verified to be one in [Bat11] with the arithmetic genus of such a curve computed in Section 3.6.1.

The main result of this chapter is an effective version of a test for arithmetically Cohen-Macaulayness (Corollary 3.3.3) which immediately yields an algorithm given the ability to numerically compute Hilbert functions up to a specified degree. The upper bound on our test is sharp, as demonstrated by the example in Section 3.6.2, which is also used to compare our new approach with that of [Hau09]. We review Hilbert functions in Section 3.2.2, and throughout this chapter we explain how they can be used

to compute certain invariants of an algebraic set. We also describe how to compute additional information in the special case that the set is a curve.

Even though it is not directly related to deciding arithmetically Cohen-Macaulayness, we note that a symbolic-numeric approach for computing Hilbert functions and Hilbert polynomials in local rings is described in [Kro13]. This approach is based on computing the Macaulay dual space of an ideal at a point that (approximately) lies in the solution set of the ideal. There are no assumptions related to the point, e.g., multiple components could pass through the point including embedded components. The practicality of this approach, especially for high dimensional components, is limited by the stopping criterion which requires that the Macaulay dual space is computed in degree up to twice the maximum degree of a "g-corner."

The rest of this chapter is organized as follows. In Section 3.2 we describe several properties of algebraic sets and introduce some of the tools we will use. Section 3.3 develops an algorithm for deciding the arithmetically Cohen-Macaulayness of a curve with Section 3.4 considering the general case. In Section 3.5 we discuss an application to physics, and in Section 3.6 we discuss other applications.

3.2 Properties and tools

3.2.1 Arithmetically Cohen-Macaulay

A positive dimensional algebraic set X with ideal sheaf $\mathcal{I}_X$ is said to be *arithmetically Cohen-Macaulay* (aCM) if

$$H^i_*(\mathcal{I}_X) = 0 \quad \text{for} \quad 1 \leq i \leq \dim X \tag{3.1}$$

where $H^i_*(\mathcal{I}_X)$ denotes the i^{th} cohomology module of $\mathcal{I}_X$. Equivalently, X is aCM if and only if its coordinate ring has Krull dimension equal to its depth [Mig98] (in this case, the coordinate ring is called a Cohen-Macaulay ring). All zero-dimensional algebraic sets are aCM, and a consequence of the above definition is that all aCM algebraic sets must be pure-dimensional.

Example 3.2.1 *Consider the curves in* $\mathbb{P}^3$*:*

$$C = \{(s^3, s^2t, st^2, t^3) \ : \ (s,t) \in \mathbb{P}^1\} \quad \textit{and} \quad Q = \{(s^4, s^3t, st^3, t^4) \ : \ (s,t) \in \mathbb{P}^1\}$$

with corresponding ideals

$$I(C) = \langle xz - y^2, yw - z^2, xw - yz \rangle \quad \textit{and} \quad I(Q) = \langle xw - yz, x^2z - y^3, xz^2 - y^2w, z^3 - yw^2 \rangle.$$

C is the twisted cubic curve which has been discussed in Section 1.1 and Example 2.4.1, while Q is a smooth rational quartic curve. The twisted cubic curve is well-known to be aCM, while Example 1.7 of [Gor06] shows that Q is not. We verify this statement using the definition by comparing the Krull dimension and depth. First, we see that both coordinate rings have Krull dimension 2*. Computations using the* `Depth` *package of Macaulay2 [GS] find that the depth of C is* 2 *and the depth of Q is* 1*.*

The cohomology characterization presented in (3.1) imposes conditions on the Hilbert function, which is defined next. For a curve, Corollary 3.3.3 presents an effective test of arithmetically Cohen-Macaulayness that can be performed using numerical algebraic geometry.

3.2.2 Hilbert functions, genus, and regularity

Let $X \subset \mathbb{P}^n$ be an algebraic set with corresponding homogeneous ideal $I \subset \mathbb{C}[x_0, \ldots, x_n]$. Let $\mathbb{C}[x_0, \ldots, x_n]_t$ denote the vector space of homogeneous polynomials of degree t, which has dimension $\binom{n+t}{t}$, and let $I_t = I \cap \mathbb{C}[x_0, \ldots, x_n]_t$. The *Hilbert function* of X is defined as

$$HF_X(t) = \begin{cases} 0 & \text{if } t < 0 \\ \binom{n+t}{t} - \dim I_t & \text{otherwise.} \end{cases} \tag{3.2}$$

The *initial degree* of X is the smallest t such that $\dim I_t > 0$. If $X = \mathbb{P}^n$, that is, $I = \langle 0 \rangle$, then the initial degree is defined as $-\infty$. If $X = \emptyset$, that is, $I = \langle 1 \rangle$, then the initial degree is 0. For all other $X \subset \mathbb{P}^n$, the initial degree is a positive integer.

Since $HF_X(t) = 0$ for $t < 0$, we will often express HF_X via the list $HF_X(0)$, $HF_X(1)$, $HF_X(2)$, ... The generating function of HF_X is called the *Hilbert series* of X, namely

$$HS_X(t) = \sum_{j=0}^{\infty} HF_X(j) \cdot t^j.$$

One key operation on Hilbert functions is taking differences, e.g., the first difference of HF_X is

$$\Delta HF_X(t) = HF_X(t) - HF_X(t-1) \quad \text{for all } t \in \mathbb{Z}.$$

By (3.2), we know $\Delta HF_X(t) = 0$ for $t < 0$ and $\Delta HF_X(0) = 1$. One can also iterate this process. For example, the k^{th} difference of HF_X is

$$\Delta^k HF_X(t) = \underbrace{\Delta \circ \cdots \circ \Delta}_{k \text{ times}} HF_X(t).$$

The Hilbert function of X becomes polynomial in t for $t \gg 0$. That is, there exists

a polynomial HP_X, called the *Hilbert polynomial* of X, such that $HF_X(t) = HP_X(t)$ for all $t \gg 0$. The Hilbert polynomial has rational coefficients with highest degree term $\frac{\deg X}{(\dim X)!} \cdot t^{\dim X}$. When X is a curve, the Hilbert polynomial of X is of the form

$$HP_X(t) = \deg X \cdot t + (1 - g_X) \tag{3.3}$$

where g_X is the *arithmetic genus* of X.

Example 3.2.2 *Consider the quartic curve $Q \subset \mathbb{P}^3$ from Ex. 3.2.1. From the generators of $I(Q)$, we compute via Macaulay2 [GS] that*

$$HF_Q = 1, 4, 9, 13, 17, 21, 25, \quad HS_Q(t) = (1+2t+2t^2-t^3)/(1-t)^2, \quad \text{and} \quad HP_Q(t) = 4t+1.$$

From HF_Q, the initial degree of Q is 2. From HP_Q and (3.3), the arithmetic genus of Q is $g_Q = 0$.

We will discuss two types of regularity for X. The *index of regularity* of X is the smallest integer ρ_X such that $HF_X(t) = HP_X(t)$ for all $t \geq \rho_X$. Let $\mathcal{I}_X$ be the sheafification of the ideal I corresponding to X. The *Castelnuovo-Mumford regularity* of X is

$$\operatorname{reg} X = \min\{m \ : \ H^i(\mathcal{I}_X(m-i)) = 0 \ \text{ for all } i > 0\}.$$

If X is aCM, then ρ_X, $\operatorname{reg} X$, and $\dim X$ are related as follows.

Proposition 3.2.3 *Suppose that $X \subset \mathbb{P}^n$ is an aCM scheme.*

1. $\operatorname{reg} X = \rho_X + \dim X + 1$.
2. *Let $\mathcal{L} \subset \mathbb{P}^n$ be a general linear space with* $\operatorname{codim} \mathcal{L} \leq \dim X$ *and $Z = X \cap \mathcal{L}$. Then* $\operatorname{reg} Z = \operatorname{reg} X$ *and* $\rho_Z = \rho_X + \operatorname{codim} \mathcal{L}$.

Proof. See, for example, Remark 2.5a of [Cio09] for Item 1. Item 2 follows immediately by combining pg. 30 of [Mig98] and Item 1. □

For aCM algebraic sets, this proposition shows that the index of regularity increases under intersection with a general hyperplane. Thus, the index of regularity can be negative so that the Hilbert polynomial has roots at negative integers. Sections 3.5.2 and 5.4.3 present examples of this.

The following will be used in Section 3.3 for computing $\operatorname{reg} C$ where $C \subset \mathbb{P}^n$ is a curve, that is, a union of irreducible one-dimensional algebraic sets.

Proposition 3.2.4 *Let $C \subset \mathbb{P}^n$ be a curve and $\mathcal{H} \subset \mathbb{P}^n$ be a general hyperplane. If $W = C \cap \mathcal{H}$, then*

$$\operatorname{reg} C = \max\{\rho_C + 1, \rho_W + 1\} = \min\{t \geq \rho_W + 1 \mid \Delta HF_C(t) = HF_W(\rho_W)\}. \tag{3.4}$$

Proof. By Lemma 2.6 of [Cio09], $\operatorname{reg} C = \max\{\rho_C + 1, \operatorname{reg} W\}$. Since $\dim W = 0$, W is aCM yielding $\operatorname{reg} W = \rho_W + 1$ by Item 1 of Prop. 3.2.3 and $HF_W(\rho_W) = \deg C$. The last equality thus follows from § 3 of [Cio09]. □

For example, using the notation of Prop. 3.2.4, if C is also aCM, then $\rho_W = \rho_C + 1$ so that

$$\operatorname{reg} W = \operatorname{reg} C = \rho_W + 1 = \rho_C + 2. \tag{3.5}$$

Example 3.2.5 *From HF_Q and HP_Q presented in Ex. 3.2.2, we have $\rho_Q = 2$. If $W = Q \cap \mathcal{H}$ for a general hyperplane $\mathcal{H} \subset \mathbb{P}^3$, then one can use [Gri14] to compute $HF_W = 1, 3, 4, 4, \ldots$ and $\rho_W = 2$. Hence,* (3.4) *yields* $\operatorname{reg} Q = 3$ *and, since* (3.5) *does not hold, this again shows Q is not aCM.*

3.2.3 Interpolation

The process by which we compute Hilbert functions relies on standard interpolation theory. To demonstrate, suppose an algebraic set $X \subset \mathbb{C}^3$ has coordinates x, y, z and we want to compute $HF_X(2)$. Using the method outlined in Section 2.4.1, we compute sample points $(x_1, y_1, z_1), \ldots, (x_r, y_r, z_r)$ lying approximately on X. In the context of elimination problems, this may involve sampling points in the fiber using a witness set and then mapping the points into the image.

We note from (3.2) that computing the Hilbert function in degree 2 only requires computing $\dim I_2$. That is, we want to compute the dimension of the vector space of degree 2 polynomials p satisfying $p(x_i, y_i, z_i) = 0$ for all sample points. Such a polynomial must be in the form

$$p(x, y, z) = a_1x^2 + a_2y^2 + a_3z^2 + a_4xy + a_5xz + a_6yz + a_7x + a_8y + a_9z + a_{10}$$

for some $a_1, \ldots, a_{10}$. Thus, we formulate the nullspace problem

$$\begin{bmatrix} x_1^2 & y_1^2 & z_1^2 & \cdots & 1 \\ \vdots & & & & \vdots \\ x_r^2 & y_r^2 & z_r^2 & \cdots & 1 \end{bmatrix} \begin{bmatrix} a_1 \\ \vdots \\ a_{10} \end{bmatrix} = \begin{bmatrix} 0 \\ \vdots \\ 0 \end{bmatrix},$$

which can be solved numerically, e.g., using MATLAB [Mat14]. In general, this nullspace problem requires $\binom{n+t}{t}$ coefficients a_i when computing $HF_X(t)$ for $X \subset \mathbb{C}^n$. Although the size of these nullspace problems grows combinatorially, we find applications for which the aCM method that follows only requires $HF_X(t)$ for relatively small t.

3.3 Computations for a curve

The following considers curves with Section 3.4 exploring higher-dimensional cases.

3.3.1 Computing invariants

Let $C \subset \mathbb{P}^n$ be a curve, that is, C is a union of one-dimensional irreducible algebraic sets. The defining equations for C may be unknown, but we assume that we have either a witness set or a pseudowitness set for each irreducible component of C, thereby providing the ability to sample points from each irreducible component of C. We also need the ability to compute $HF_C(t)$ as described in Section 3.2.3.

For a curve $C \subset \mathbb{P}^n$, six invariants of interest are the Castelnuovo-Mumford regularity, index of regularity, arithmetic genus, geometric genus, Hilbert polynomial, and Hilbert series. The geometric genus can be computed using [Bat11] from a witness set for C. The following uses the ability to compute $HF_C(t)$ via the method of Section 3.2.3 given HF_W and ρ_W, both of which can be computed via [Gri14], to compute the other five invariants.

3.3.1.1 Castelnuovo-Mumford regularity

The Castelnuovo-Mumford regularity $\operatorname{reg} C$ is derived from (3.4) by using the method of Section 3.2.3 to compute enough terms of HF_C.

3.3.1.2 Hilbert polynomial, arithmetic genus, and index of regularity

If $\operatorname{reg} C > \rho_W + 1$, then (3.4) also yields $\rho_C = \operatorname{reg} C - 1$. Thus, $HF_C(\rho_C) = HP_C(\rho_C)$ so that (3.3) yields

$$g_C = \deg C \cdot \rho_C - HF_C(\rho_C) + 1 = HP_W(\rho_W) \cdot \rho_C - HF_C(\rho_C) + 1 \tag{3.6}$$

$$HP_C(t) = \deg C \cdot t + (1 - g_C) = HP_W(\rho_W) \cdot t + (HF_C(\rho_C) - HP_W(\rho_W) \cdot \rho_C). \tag{3.7}$$

If $\operatorname{reg} C \leq \rho_W + 1$, then (3.4) yields $\rho_C \leq \rho_W$. Since $HF_C(\rho_W) = HP_C(\rho_W)$, (3.3) yields

$$g_C = \deg C \cdot \rho_W - HF_C(\rho_W) + 1 = HP_W(\rho_W) \cdot \rho_W - HF_C(\rho_W) + 1 \tag{3.8}$$

$$HP_C(t) = \deg C \cdot t + (1 - g_C) = HP_W(\rho_W) \cdot t + (HF_C(\rho_W) - HP_W(\rho_W) \cdot \rho_W). \tag{3.9}$$

In this case, $\rho_C = \min\{-1 \leq t \leq \rho_W \mid HF_C(t) = HP_C(t)\}$.

3.3.1.3 Hilbert series

By adapting p. 28 of [Mig98] to this situation, we have

$$HS_C(t) = \frac{\sum_{j=0}^{\rho_C+1} \Delta^2 HF_C(j) \cdot t^j}{(1-t)^2}. \tag{3.10}$$

Example 3.3.1 *Consider the degree* 8 *curve in* $\mathbb{P}^3$ *derived from Ex. 1.7 of [Gor06]:*

$$C = \{(s^8, s^7t, st^7, t^8) \mid (s,t) \in \mathbb{P}^1\}.$$

We can verify that the corresponding ideal is

$$I(C) = \langle xw - yz, x^6z - y^7, x^5z^2 - y^6w, x^4z^3 - y^5w^2, x^3z^4 - y^4w^3, x^2z^5 - y^3w^4, xz^6 - y^2w^5, z^7 - yw^6 \rangle.$$

Let $\mathcal{H}$ be a general hyperplane and $W = C \cap \mathcal{H}$. Using [Gri14], we find that

$$HF_W = 1, 3, 5, 7, 8, 8 \ \text{ and } \ \rho_W = 4.$$

Using interpolation, we find that

$$HF_C = 1, 4, 9, 16, 25, 36, 49, 57, \ \Delta HF_C = 1, 3, 5, 7, 9, 11, 13, 8, \ \Delta^2 HF_C = 1, 2, 2, 2, 2, 2, 2, -5.$$

Hence, $\operatorname{reg} C = 7$ *and* $\rho_C = \operatorname{reg} C - 1 = 6$. *Additionally,* (3.6), (3.7), *and* (3.10) *yield*

$$g_C = 8 \cdot 6 - 49 + 1 = 0, \ HP_C(t) = 8t + 1, \ HS_C(t) = \frac{1 + 2t + 2t^2 + 2t^3 + 2t^4 + 2t^5 + 2t^6 - 5t^7}{(1-t)^2}.$$

The geometric genus of a curve is the arithmetic genus of the desingularization of the curve. Since the curve in Ex. 3.3.1 is smooth, its geometric genus is equal to its arithmetic genus, namely 0. Section 3.6.1 compares these genera on a nonsmooth curve.

3.3.2 Testing arithmetically Cohen-Macaulayness of a curve

The following tests the arithmetically Cohen-Macaulayness of a curve.

Theorem 3.3.2 *Let $C \subset \mathbb{P}^n$ be a curve, $\mathcal{H} \subset \mathbb{P}^n$ be a general hyperplane, and $W = C \cap \mathcal{H}$. Then, C is aCM if and only if $\Delta HF_C(t) = HF_W(t)$ for all $t \geq 0$.*

Proof. Since C is a curve, C is aCM if and only if $H^1_*(\mathcal{I}_C) = 0$. By Prop. 1.3.4 of [Mig98], this is equivalent to $J = I(C) + \langle \ell \rangle$ being a saturated ideal in $R := \mathbb{C}[x_0, \ldots, x_n]$ where

$\mathcal{H} = \mathcal{V}(\ell)$. That is, C is aCM if and only if $J = I(W)$. Since $J \subset I(W)$, this is equivalent to $HF_{R/J}(t) = HF_W(t)$ for all $t \geq 0$. The result now follows since $HF_{R/J}(t) = \Delta HF_C(t)$ because C is a curve. $\square$

The following is a so-called *effective version* of Theorem 3.3.2.

Corollary 3.3.3 *Let $C \subset \mathbb{P}^n$ be a curve, $\mathcal{H} \subset \mathbb{P}^n$ be a general hyperplane, and $W = C \cap \mathcal{H}$. Then, C is aCM if and only if $\Delta HF_C(t) = HF_W(t)$ for all $1 \leq t \leq \rho_W + 1$.*

Proof. We know $\Delta HF_C(0) = HF_W(0) = 1$ and $HF_W(\rho_W) = HF_W(\rho_W + t)$ for all $t \geq 0$. If $\Delta HF_C(\rho_W + 1) = HF_W(\rho_W + 1) = HF_W(\rho_W)$, then $\rho_C + 1 \leq \rho_W + 1$ so that $\rho_C \leq \rho_W$. Hence, $HP_C(\rho_W + t) = HF_C(\rho_W + t)$ for all $t \geq 0$ which yields

$$\Delta HF_C(\rho_W + t) = HF_W(\rho_W + t) = HF_W(\rho_W) \text{ for all } t \geq 1.$$

In particular, we have shown that $\Delta HF_C(t) = HF_W(t)$ for $1 \leq t \leq \rho_W + 1$ is equivalent to $\Delta HF_C(t) = HF_W(t)$ for all $t \geq 0$. Therefore, the statement holds by Theorem 3.3.2. $\square$

Section 3.6.2 provides an example that is not aCM such that $\Delta HF_C(t) = HF_W(t)$ for all $1 \leq t \leq \rho_W$. Hence, the effective upper bound of $\rho_W + 1$ provided in Corollary 3.3.3 is sharp.

Corollary 3.3.3 immediately yields an algorithm for determining whether or not a curve C is arithmetically Cohen-Macaulay. As discussed in Section 3.2.3, [Gri14] can be used to compute both HF_W and ρ_W, where W is a general hyperplane section of C, upon fixing a general affine patch. Additionally, interpolation can be used to compute $HF_C(1), \ldots, HF_C(\rho_W + 1)$ with $HF_C(0) = 1$. Thus, C is aCM if and only if $HF_C(t) - HF_C(t-1) = HF_W(t)$ for $t = 1, \ldots, \rho_W + 1$.

Example 3.3.4 *Recall the curves C and Q in $\mathbb{P}^3$ from Ex. 3.2.1. Let $\mathcal{H}$ be a general hyperplane, $W_C = C \cap \mathcal{H}$, and $W_Q = Q \cap \mathcal{H}$. For the twisted cubic curve C, we compute*

$$HF_{W_C} = 1, 3, 3, \quad \rho_{W_C} = 1, \quad HF_C = 1, 4, 7, \quad \Delta HF_C = 1, 3, 3.$$

Since $\Delta HF_C(t) = HF_{W_C}(t)$ for $1 \leq t \leq \rho_{W_C} + 1 = 2$, Corollary 3.3.3 shows that C is aCM.

Similarly, for the quartic curve Q, we compute

$$HF_{W_Q} = 1, 3, 4, 4, \quad \rho_{W_Q} = 2, \quad HF_Q = 1, 4, 9, 13, \quad \Delta HF_Q = 1, 3, 5, 4.$$

Since $\Delta HF_Q(2) = 5 \neq 4 = HF_{W_Q}(2)$, Corollary 3.3.3 shows that Q is not aCM.

3.4 Higher-dimensional cases

3.4.1 Testing arithmetically Cohen-Macaulayness

The key to testing the arithmetically Cohen-Macaulayness of an algebraic set of dimension at least 2 is to test the arithmetically Cohen-Macaulayness of a general curve section.

Theorem 3.4.1 *Let $X \subset \mathbb{P}^n$ be a pure-dimensional algebraic set of dimension $d > 1$ and $\mathcal{L} \subset \mathbb{P}^n$ be a general linear space of codimension $d - 1$. Then, X is aCM if and only if the curve $X \cap \mathcal{L}$ is aCM.*

Proof. If X is aCM, then Theorem 1.3.3 of [Mig98] yields that $X \cap \mathcal{L}$ is also aCM. Conversely, if the projective curve $X \cap \mathcal{L}$ is aCM, then Prop. 2.1 of [HU93] provides that X must also be aCM. □

The combination of Theorem 3.4.1 and Corollary 3.3.3 yields a test for deciding the arithmetically Cohen-Macaulayness of a pure-dimensional algebraic set of dimension at least 2 by determining the arithmetically Cohen-Macaulayness of a general curve section. Additional information about this general curve section can be computed via Section 3.3.1, such as its arithmetic genus.

Example 3.4.2 *Let $X \subset \mathbb{P}^4$ be the degree 4 surface defined by the ideal*

$$I = \langle x_0x_1 - x_2^2, x_0x_3 - x_4^2 \rangle \subset \mathbb{C}[x_0, x_1, x_2, x_3, x_4].$$

Let $\mathcal{L}$ and $\mathcal{H}$ be general hyperplanes with $C = X \cap \mathcal{L}$ and $W = C \cap \mathcal{H}$. Since

$$HF_W = 1, 3, 4, 4, \quad \rho_W = 2, \quad HF_C = 1, 4, 8, 12, \quad \Delta HF_C = 1, 3, 4, 4,$$

Corollary 3.3.3 yields that C is aCM so that X is aCM by Theorem 3.4.1.

If $X \subset \mathbb{P}^n$ is aCM of dimension $d > 1$ and $W \subset \mathbb{P}^n$ is a general linear section of complimentary dimension, then the index of regularity of X and Castelnuovo-Mumford regularity of X can be computed directly from the index of regularity of W via Prop. 3.2.3. The remainder of this section describes how to compute the Hilbert function, Hilbert series, and Hilbert polynomial of X given the Hilbert function and index of regularity of W.

3.4.1.1 Hilbert function

Using Corollary 1.3.8(d) of [Mig98] applied d times, we have

$$\Delta^d HF_X(t) = HF_W(t) \text{ for all } t \geq 0.$$

In particular, unrolling this formula provides

$$HF_X(t) = \sum_{j_1=0}^{t} \sum_{j_2=0}^{j_1} \cdots \sum_{j_d=0}^{j_{d-1}} HF_W(j_d). \tag{3.11}$$

3.4.1.2 Hilbert series

By adapting pg. 28 of [Mig98] to this situation, we have

$$HS_X(t) = \frac{\sum_{j=0}^{\rho_W} \Delta^{d+1} HF_X(j) \cdot t^j}{(1-t)^{d+1}} = \frac{\sum_{j=0}^{\rho_W} \Delta HF_W(j) \cdot t^j}{(1-t)^{d+1}}. \tag{3.12}$$

3.4.1.3 Hilbert polynomial

Since $HP_X(t)$ is a polynomial of degree d with rational coefficients and $HP_X(\rho_X + j) = HF_X(\rho_X + j)$ for all $j \geq 0$, standard polynomial interpolation computes HP_X.

Example 3.4.3 *Let $X \subset \mathbb{P}^4$ be the surface from Ex. 3.4.2, which is aCM. From Prop. 3.2.3 and* (3.5),

$$\rho_C = 1, \quad \rho_X = 0, \quad \operatorname{reg} X = 3.$$

Following (3.11) *and* (3.12) *with data from Ex. 3.4.2, we have*

$$HF_X(t) = 1, 5, 13, 25, 41, 61, \ldots \quad \textit{and} \quad HF_S(t) = \frac{1 + 2t + t^2}{(1-t)^3}.$$

Interpolation yields $HP_X(t) = 2t^2 + 2t + 1$.

3.4.2 Minimal generators

Let $I \subset \mathbb{C}[x_0, \ldots, x_n]$ be a homogeneous ideal. For each $j \geq 0$, there exists $d_j(I) \geq 0$ such that every minimal generating set consisting of homogeneous polynomials for I consists of exactly $d_j(I)$ polynomials of degree j. For an algebraic set $X \subset \mathbb{P}^n$, $d_j(X)$ is defined as $d_j(I)$ where I is the corresponding homogeneous ideal. In fact, $d_j(X) = 0$ for $j > \operatorname{reg} X$. When X is arithmetically Cohen-Macaulay, the following provides an approach to compute $d_j(X)$.

Proposition 3.4.4 *Let $X \subset \mathbb{P}^n$ be an arithmetically Cohen-Macaulay scheme of dimension $d > 0$, $\mathcal{L} \subset \mathbb{P}^n$ be a general linear space of codimension $0 < \ell \leq d$, and $Z = X \cap \mathcal{L} \subset \mathcal{L}$. Then, $d_j(X) = d_j(Z)$ for all j. In particular, the initial degree of X is the initial degree of Z.*

Proof. By treating Z as a subscheme of $\mathcal{L}$, the result follows from Theorem 1.3.6 of [Mig98]. □

Example 3.4.5 *Let $X \subset \mathbb{P}^4$ be the aCM surface introduced in Ex. 3.4.2. By looking at the generating set of the ideal, one sees $d_2(X) = 2$ with $d_j(X) = 0$ for all other j. Thus, by Prop. 3.4.4, we have $d_2(W) = 2$ with $d_j(W) = 0$ for all other j. This can be verified directly by performing computations on W as follows. We have $d_0(W) = 0$ and, since $\operatorname{reg} W = 3$, $d_j(W) = 0$ for $j \geq 4$. Since $HF_W(1) = \binom{2+1}{1}$ and $HF_W(2) = \binom{2+2}{2} - 2$, we know $d_1(W) = 0$ and $d_2(W) = 2$. Using linear algebra, we find that this two dimensional space of quadratic polynomials generates a six dimensional space of cubic polynomials. Since $HF_W(3) = \binom{2+3}{3} - 6$, $d_3(W) = 0$.*

3.5 An application to physics

3.5.1 Statement of the problem

An open question in theoretical physics is the nature of the vacuum space in the Minimal Supersymmetric Standard Model (MSSM) [Gra06]. This gives rise to a family of problems that can be written as polynomial images of algebraic sets. In [Gra06], many of these problems were studied symbolically using Macaulay2, but some were found to be impractical. In these sections, we discuss an ongoing investigation into these image sets using numerical elimination theory.

These elimination problems arise due to a superpotential in the MSSM containing operators which represent different particle interactions. In our work we consider 9 such operators, each of which can either be present or absent from the model. Thus, we consider $2^9 = 512$ different scenarios. An open question is whether certain phenomenology in physics correlates to certain geometry in these image sets. To investigate this, we want to compute properties in as many scenarios as possible. Specifically, we are given 512 polynomial maps $G_1, \ldots, G_{512}$, where each G_i maps from $\mathbb{C}^{16} \to \mathbb{C}^{16}$. We are given one map $\pi : \mathbb{C}^{16} \to \mathbb{C}^{25}$, and our objects of interest are the image sets $\overline{\pi(V(G_i))}$ for $i = 1, \ldots, 512$. Although many of these sets were successfully analyzed in [Gra06], we perform our numerical computations for all 512 problems to demonstrate the effectiveness of our approach.

3.5.2 A close look at one system

In this section, we take a close look at one scenario. In Section 3.5.3, we summarize the results from all 512 problems.

Let $G : \mathbb{C}^{16} \to \mathbb{C}^{16}$ be defined by

$$
\begin{aligned}
g_1 &= 6x_{11}x_4 + 2x_{13}x_4 - 6x_{10}x_5 - 2x_{12}x_5 - 4x_5x_8 + 4x_4x_9 \\
g_2 &= 6x_{10}x_3 + 2x_{12}x_3 - 3x_{14}x_6 - x_{15}x_6 - 4x_{16}x_6 + 4x_3x_8 + 3x_2x_{10} + 3x_2x_{12} + 8x_2x_8 \\
&\quad +2x_1x_{10} + 5x_1x_{12} + 10x_1x_8 \\
g_3 &= 10x_1x_5 + 8x_2x_5 + 4x_3x_5 \\
g_4 &= 6x_{11}x_3 + 2x_{13}x_3 - 3x_{14}x_7 - x_{15}x_7 - 4x_{16}x_7 + 2x_1x_{11} + 5x_1x_{13} + 10x_1x_9 + 3x_2x_{11} \\
&\quad +3x_2x_{13} + 8x_2x_9 + 4x_3x_9 \\
g_5 &= 10x_1x_4 + 8x_2x_4 + 4x_3x_4 \\
g_6 &= 2x_1x_5 + 3x_2x_5 + 6x_3x_5 \\
g_7 &= 2x_1x_4 + 3x_2x_4 + 6x_3x_4 \\
g_8 &= 5x_1x_5 + 3x_2x_5 + 2x_3x_5 \\
g_9 &= 5x_1x_4 + 3x_2x_4 + 2x_3x_4 \\
g_{10} &= 2x_5x_{10} + 5x_5x_{12} + 10x_5x_8 - 2x_4x_{11} - 5x_4x_{13} - 10x_4x_9 \\
g_{11} &= 3x_5x_{10} + 3x_5x_{12} + 8x_5x_8 - 3x_4x_{11} - 3x_4x_{13} - 8x_4x_9 \\
g_{12} &= 3x_{14}x_5 + x_{15}x_5 + 4x_{16}x_5 \\
g_{13} &= 2x_{14} + 6x_{14}^2 + 3x_{15} + 4x_{14}x_{15} + 8x_{15}^2 + 10x_{16} + 16x_{14}x_{16} + x_{15}x_{16} + 3x_{16}^2 - 3x_5x_6 + 3x_4x_7 \\
g_{14} &= 3x_{14}x_4 + x_{15}x_4 + 4x_{16}x_4 \\
g_{15} &= 3x_{14} + 2x_{14}^2 + 6x_{15} + 16x_{14}x_{15} + 3x_{15}^2 + 2x_{16} + x_{14}x_{16} + 4x_{15}x_{16} + 4x_{16}^2 - x_5x_6 + x_4x_7 \\
g_{16} &= 10x_{14} + 8x_{14}^2 + 2x_{15} + x_{14}x_{15} + 2x_{15}^2 + 4x_{16} + 6x_{14}x_{16} + 8x_{15}x_{16} + 27x_{16}^2 - 4x_5x_6 + 4x_4x_7
\end{aligned}
$$

and let $\pi : \mathbb{C}^{16} \to \mathbb{C}^{25}$ be

$$
\begin{aligned}
\pi_1 &= x_{14} & \pi_{14} &= x_1x_{11}x_{12} - x_1x_{10}x_{13}\\
\pi_2 &= x_{15} & \pi_{15} &= x_2x_{11}x_{12} - x_2x_{10}x_{13}\\
\pi_3 &= x_{16} & \pi_{16} &= x_3x_{11}x_{12} - x_3x_{10}x_{13}\\
\pi_4 &= x_7x_8 - x_6x_9 & \pi_{17} &= x_1x_5x_8 - x_1x_4x_9\\
\pi_5 &= x_7x_{10} - x_6x_{11} & \pi_{18} &= x_2x_5x_8 - x_2x_4x_9\\
\pi_6 &= x_7x_{12} - x_6x_{13} & \pi_{19} &= x_3x_5x_8 - x_3x_4x_9\\
\pi_7 &= x_5x_6 - x_4x_7 & \pi_{20} &= x_1x_5x_{10} - x_1x_4x_{11}\\
\pi_8 &= x_1x_9x_{10} - x_1x_8x_{11} & \pi_{21} &= x_2x_5x_{10} - x_2x_4x_{11}\\
\pi_9 &= x_2x_9x_{10} - x_2x_8x_{11} & \pi_{22} &= x_3x_5x_{10} - x_3x_4x_{11}\\
\pi_{10} &= x_3x_9x_{10} - x_3x_8x_{11} & \pi_{23} &= x_1x_5x_{12} - x_1x_4x_{13}\\
\pi_{11} &= x_1x_9x_{12} - x_1x_8x_{13} & \pi_{24} &= x_2x_5x_{12} - x_2x_4x_{13}\\
\pi_{12} &= x_2x_9x_{12} - x_2x_8x_{13} & \pi_{25} &= x_3x_5x_{12} - x_3x_4x_{13}\\
\pi_{13} &= x_3x_9x_{12} - x_3x_8x_{13}
\end{aligned}
$$

Consider the algebraic set $A = \overline{\pi(V(G))} \subset \mathbb{C}^{25}$. An attempt using Macaulay2 to symbolically perform the elimination was unsuccessful after running for 4 weeks. Using the approach presented in [Hau13b] and `Bertini`, we find that A has 11 irreducible components, namely $Y_1, \ldots, Y_8$ each of dimension 5 and degree 6, and 3 three-dimensional linear spaces. We let $Y_1, \ldots, Y_4$ denote the self-conjugate ones whereas Y_6 and Y_8 are conjugate to Y_5 and Y_7, respectively. For $j = 1, \ldots, 8$, let $X_j \subset \mathbb{P}^{25}$ be the closure of the image of Y_j under the map $\mathbb{C}^{25} \hookrightarrow \mathbb{P}^{25}$ defined by $x \to (1, x)$.

We first investigate the arithmetically Cohen-Macaulayness of each X_j. After selecting a random linear space $\mathcal{L} \subset \mathbb{P}^{25}$ of codimension 4 and a random hyperplane $\mathcal{H} \subset \mathbb{P}^{25}$, we

compute the following for each $C_j = X_j \cap \mathcal{L}$ and $W_j = C_j \cap \mathcal{H}$:

$$HF_{W_j} = 1, 5, 6, 6, \quad HF_{C_j} = 1, 6, 12, 18, \quad \Delta HF_{C_j} = 1, 5, 6, 6.$$

Thus, Corollary 3.3.3 and Theorem 3.4.1 yield C_j and X_j are aCM for each $j = 1, \ldots, 8$. In particular, $\operatorname{reg} X_j = \operatorname{reg} C_j = \operatorname{reg} W_j = 3$, $\rho_{C_j} = 1$, $\rho_{X_j} = -3$, and (3.8) yields $g_{C_j} = 1$.

Using Prop. 3.4.4, we can describe the minimal generators of X_j via W_j. For $k > \operatorname{reg} X_j = 3$, we know $d_k(X_j) = 0$. By treating $W_j \subset \mathcal{L} \cap \mathcal{H}$, $HF_{W_j}(1) = \binom{20+1}{1} - 5 = 16$ implies that $d_1(X_j) = d_1(W_j) = 16$. By additionally restricting to this 16 dimensional linear space, we know $d_2(X_j) = d_2(W_j) = 9$ since $HF_{W_j}(2) = \binom{4+2}{2} - 9 = 6$. Moreover, since these quadratics generate a 29 dimensional space of cubics with $HF_{W_j}(3) = \binom{4+3}{3} - 29 = 6$, $d_3(X_j) = d_3(W_j) = 0$. Therefore, each X_j is minimally generated over $\mathbb{C}$ by 16 linear and 9 quadratic polynomials with

$$\begin{aligned}
HP_{C_j}(t) &= 6t & HS_{C_j}(t) &= (1 + 4t + t^2)/(1 - t)^2 \\
HF_{X_j} &= 1, 10, 46, 146, 371, \ldots & HS_{X_j}(t) &= (1 + 4t + t^2)/(1 - t)^6 \\
HP_{X_j}(t) &= 1/20 \cdot t^5 + 1/2 \cdot t^4 + 23/12 \cdot t^3 + 7/2 \cdot t^2 + 91/30 \cdot t + 1 \\
&= \tfrac{3 \cdot t^2 + 12 \cdot t + 10}{60} \textstyle\prod_{j=1}^{3} (t + j).
\end{aligned}$$

Next, we investigate the $\mathbb{R}$-irreducible components $X_5 \cup X_6$ and $X_7 \cup X_8$. Since

$$HF_{W_j \cup W_{j+1}} = 1, 9, 12, 12, \quad HF_{C_j \cup C_{j+1}} = 1, 10, 24, 36, \quad \Delta HF_{C_j \cup C_{j+1}} = 1, 9, 14, 12$$

for $j = 5$ and $j = 7$, $X_5 \cup X_6$ and $X_7 \cup X_8$ are not aCM.

Finally, we test the arithmetically Cohen-Macaulayness of $X = X_1 \cup \cdots \cup X_8$ by considering $C = C_1 \cup \cdots \cup C_8$ and $W = W_1 \cup \cdots \cup W_8$. Since $HF_W(1) = 11 \neq 13 =$

$\Delta HF_C(1)$, X is not aCM.

3.5.3 Summary of results

For each of the 512 scenarios, we performed a numerical irreducible decomposition of the image set, with the exception of 42 scenarios for which we find $V(G) = \emptyset$. Altogether, we found 2730 irreducible components. For each component, we computed the dimension, degree, Hilbert function, Hilbert polynomial, and Hilbert series. The dimensions ranged from 0 to 10, and the degrees ranged from 1 to 56.

We have also begun analyzing additional scenarios which consider different choices of particle interactions. In a preliminary investigation of 256 such problems, we found 484 irreducible components and computed the same properties mentioned above. In these cases, the dimensions range from 0 to 13 and the degrees ranged from 1 to 1872.

As of the time of this writing, we are investigating other variations of the model while these results are interpreted for physical significance.

3.6 Other applications

3.6.1 The coupler curve of a planar four-bar linkage

Since the curve in Ex. 3.3.1 was smooth, its arithmetic genus and geometric genus are equal. Here, we investigate a nonsmooth curve arising in kinematics. In particular, the coupler curve of a planar four-bar linkage describes the motion allowed by a mechanism consisting of four hinged bars arranged as a quadrilateral in the plane. The arrangement

of the mechanism is described by ten parameters $(p, \overline{p}, q, \overline{q}, s, \overline{s}, t, \overline{t}, r, R) \in \mathbb{C}^{10}$. If

$$a_1 = s(\overline{z} - \overline{p}), \quad \overline{a}_1 = \overline{s}(z - p), \quad \alpha_1 = (z - p)(\overline{z} - \overline{p}) + s\overline{s} - r,$$
$$a_2 = t(\overline{z} - \overline{q}), \quad \overline{a}_2 = \overline{t}(z - q), \quad \alpha_2 = (z - q)(\overline{z} - \overline{q}) + t\overline{t} - R,$$

then the coupler curve is the set of points $(z, \overline{z}) \in \mathbb{C}^2$ satisfying

$$\begin{vmatrix} \overline{a}_1 & \alpha_1 \\ \overline{a}_2 & \alpha_2 \end{vmatrix} \cdot \begin{vmatrix} a_1 & \alpha_1 \\ a_2 & \alpha_2 \end{vmatrix} + \begin{vmatrix} a_1 & \overline{a}_1 \\ a_2 & \overline{a}_2 \end{vmatrix}^2 = 0. \tag{3.13}$$

By fixing random values for the parameters and homogenizing (3.13), we will treat a general coupler curve C as a projective algebraic set in $\mathbb{P}^2$. The degree of C is 6, and the numerical algebraic geometry approach of [Bat11] verified that the geometric genus is 1.

Let $W = C \cap \mathcal{H}$ where $\mathcal{H} \subset \mathbb{P}^2$ is a random hyperplane. Then

$$HF_W = 1, 2, 3, 4, 5, 6, 6, \quad HF_C = 1, 3, 6, 10, 15, 21, 27, \quad \Delta HF_C = 1, 2, 3, 4, 5, 6, 6$$

shows that C is aCM by Corollary 3.3.3. In particular, from (3.8) we determine that the arithmetic genus is $g_C = 10$.

3.6.2 A non-aCM example

Consider the map $\pi : \mathbb{C}^4 \times \mathbb{C}^4 \times \mathbb{C}^4 \times \mathbb{C}^4 \to \mathbb{C}^{16}$ defined by

$$(\mathbf{s}, \mathbf{t}, \mathbf{u}, \mathbf{v}) \mapsto s_{k\ell} t_{ij} + u_{ik} v_{j\ell} \text{ for } i, j, k, \ell = 1, 2.$$

Let $Y = \overline{\pi(\mathbb{C}^4 \times \mathbb{C}^4 \times \mathbb{C}^4 \times \mathbb{C}^4)} \subset \mathbb{C}^{16}$. Our object of interest is the projectivization of Y, which we will denote by $X = \mathbb{P}(Y) \subset \mathbb{P}^{15}$. Using π, we compute $\dim X = 13$. After selecting a random linear space $\mathcal{L} \subset \mathbb{P}^{15}$ of codimension 12 and random hyperplane $\mathcal{H} \subset \mathbb{P}^{15}$, consider the curve $C = X \cap \mathcal{L}$ and witness point set $W = C \cap \mathcal{H}$. We use `Bertini` to compute W and a pseudowitness set [HS10] for C which yields $\deg X = 28$. Interpolation and [Gri14] produces

$$HF_W = 1, 3, 6, 10, 15, 21, 28, 28$$
$$HF_C = 1, 4, 10, 20, 35, 56, 84, 120$$
$$\Delta HF_C = 1, 3, 6, 10, 15, 21, 28, 36.$$

In particular, $\rho_W = 6$ with $\Delta HF_C(7) = 36 \neq 28 = HF_W(7)$ which yields that C is not aCM. Therefore, by Theorem 3.4.1, X is not aCM.

For this non-aCM example, the terms of HF_C computed while testing C for arithmetically Cohen-Macaulayness are not enough to determine ρ_C. Since $\operatorname{reg} C > \rho_W + 1$, we use (3.4) to compute $\operatorname{reg} C$ with $\rho_C = \operatorname{reg} C - 1$. The additional terms of HF_C needed are

$$HF_C = 1, 4, 10, 20, 35, 56, 84, 120, 165, 196, 224, \ \Delta HF_C = 1, 3, 6, 10, 15, 21, 28, 36, 45, 31, 28$$

showing that $\operatorname{reg} C = 10$ with $\rho_C = 9$. Using (3.6), the arithmetic genus of C is $g_C = 57$ with

$$HP_C(t) = 28t - 56$$
$$HS_C(t) = (1 + 2t + 3t^2 + 4t^3 + 5t^4 + 6t^5 + 7t^6 + 8t^7 + 9t^8 - 14t^9 - 3t^{10})/(1 - t)^2.$$

For comparison, consider Algorithm 2.4 of [Hau09] for numerically testing the arith-

metically Cohen-Macaulayness of C. This test requires an *a priori* bound on $\operatorname{reg} C$. One could use (3.4) to compute $\operatorname{reg} C$ exactly. However, this computation provides enough data needed to use Corollary 3.3.3 to decide the arithmetically Cohen-Macaulayness of C. Alternatively, one could bound $\operatorname{reg} C$, for example, by using [Gru83] to conclude that $\operatorname{reg} C \leq 28 + 2 - 3 = 27$. In any event, if $r \geq \operatorname{reg} C$ is the selected bound, Algorithm 2.4 of [Hau09] requires computing $HF_C(r-1)$. Additionally, Algorithm 2.4 of [Hau09] also requires computing $HF_{C\cap F}(r-1)$ where F is a general form of degree at most $r-1$. Using $r = 27$ from [Gru83], one at least needs to compute $HF_C(26)$ and $HF_{C\cap F}(26)$ where F is a general form of degree 26, that is, $C \cap F$ is a zero-dimensional scheme of degree $28 \cdot 26 = 728$. Two advantages of using Corollary 3.3.3 are that the zero-dimensional scheme under consideration arises as a general hyperplane section of C rather than a general hypersurface section of C of possibly high degree and that $HF_C(t)$ is only needed up to $\rho_W + 1$ with $\rho_W + 1 \leq \operatorname{reg} C \leq r$.

Chapter 4

Investigating discriminant loci

4.1 Introduction

Consider the following polynomial equation in one variable x depending on parameters a, b, and c:

$$f(x; a, b, c) = ax^2 + bx + c = 0.$$

For a generic choice of $(a, b, c) \in \mathbb{C}^3$, this equation has 2 distinct complex solutions. However, for special parameter choices $(a, b, c) \in \mathbb{C}^3$, the equation has 0 or 1 complex solution. For example, $(a, b, c) = (1, -2, 1)$ results in $f(x; a, b, c) = (x - 1)^2$, which has a double root at $x = 1$.

Continuing with the above example, we consider the system

$$F(x; a, b, c) = \begin{bmatrix} f(x; a, b, c) \\ \frac{d}{dx} f(x; a, b, c) \end{bmatrix} = \begin{bmatrix} ax^2 + bx + c \\ 2ax + b \end{bmatrix} = 0.$$

To find special points in the parameter space, we want to eliminate x from $F(x; a, b, c) = 0$.

Let $\pi : \mathbb{C}^4 \to \mathbb{C}^3$ be the projection defined by $\pi(x, a, b, c) = (a, b, c)$. The *discriminant locus* or *discriminant variety* is the set

$$X = \overline{\pi(V(F))} \subset \mathbb{C}^3.$$

Thus, we can view the discriminant locus as an image of an algebraic set under a linear map. Using elimination theory, one can verify that $X = V(b^2 - 4ac)$.

More generally, given a polynomial system $G(x; a) = 0$ in variables $x = (x_1, \ldots, x_n)$ depending on parameters $a = (a_1, \ldots, a_\ell)$, we construct the system

$$F(x; a) = \begin{bmatrix} G(x; a) \\ \det J_x G(x; a) \end{bmatrix} = 0, \tag{4.1}$$

where we write $J_x G$ to indicate that the Jacobian of G is taken with respect to x only. Note that $\det J_x G(x; a) = 0$ when $J_x G$ is singular, so solutions to $F(x; a) = 0$ are solutions to $G(x; a) = 0$ for which nongeneric behavior occurs. To obtain points in the parameter space we must eliminate x, so we let $\pi : \mathbb{C}^{n+\ell} \to \mathbb{C}^\ell$ be the projection defined by $\pi(x, a) = a$. The discriminant locus is the set

$$X = \overline{\pi(V(F))} \subset \mathbb{C}^\ell.$$

Although finding defining equations for a discriminant locus is not always practical, we will show that valuable information can be found numerically.

4.2 The Kuramoto model

The following covers most of the material found in [Meh15], with Section 4.2.7 presenting a new algorithm to expand this work.

4.2.1 Description of the model

The Kuramoto model was proposed in 1975 to study synchronization phenomena among coupled oscillators [Kur75]. The state of an oscillator at time t, denoted $\theta(t)$, is called its *phase* and is defined to have range $[0, 2\pi)$. The rate of change $\frac{d\theta}{dt}$ is called the *frequency* of the oscillator. Given N coupled oscillators with phases $\theta_1, \ldots, \theta_N$, the Kuramoto model describes the behavior of the network via the following system of ordinary differential equations:

$$\frac{d\theta_i}{dt} = \omega_i - \frac{K}{N} \sum_{j=1}^{N} a_{i,j} \sin(\theta_i - \theta_j), \text{ for } i = 1, ..., N, \tag{4.2}$$

where K is the coupling strength, $\Omega = (\omega_1, \ldots, \omega_N)$ is the vector of intrinsic natural frequencies, and $a_{i,j} \in \{0, 1\}$ is the (i, j)th element of the adjacency matrix of the coupling graph. The natural frequencies ω_i indicate how the oscillators would behave in the absence of any coupling or external forces. We assume that the coupling graph is undirected and that the natural frequencies satisfy $\sum_{i=1}^{N} \omega_i = 0$. We will see that an interesting discriminant locus problem arises which we will approach using numerical algebraic geometry. As a byproduct of our numerical investigation into this discriminant locus problem, we will also encounter new results regarding equilibria of the Kuramoto model.

Since the Kuramoto model's introduction in 1975 [Kur75], it has gained attention from various scientific communities, including biology, chemistry, physics, and electrical engineering, due to its applicability. This model has been used to study various phenomena

including neural networks, chemical oscillators, Josephson junctions and laser arrays, power grids, particle coordination, spin glass models, and rhythmic applause [Ace05; Str00; DB14].

A system of coupled phase oscillators is said to be at *frequency synchronization* if there is a constant c such that $\frac{d\theta_i}{dt} = c$ for all i. In this case, system (4.2) yields $c = \frac{1}{N}\sum_{i=1}^{N}\omega_i$. If $c \neq 0$, then we can rotate the problem by increasing (or decreasing) all of the natural frequencies ω_i by the same amount so that $c = 0$. Thus, in the discussion that follows, we investigate synchronization by computing equilibria of the system.

Since we are working with undirected coupling graphs, i.e., $a_{i,j} = a_{j,i}$ for all i, j, we point out that the equilibria of system (4.2) can also be viewed as the stationary points of the potential energy landscape drawn by the mean-field XY model with an exogeneous perturbation term:

$$V(\theta) = \frac{K}{2N}\sum_{i,j=1}^{N} a_{i,j}(1 - \cos(\theta_i - \theta_j)) - \sum_{i=1}^{N}\omega_i\theta_i, \tag{4.3}$$

whose gradient reproduces the right-hand side of equation (4.2). Hence, in the following, we use the words equilibria and stationary points interchangeably.

All stationary points of the finite N mean-field XY model (i.e., the Kuramoto model with homogeneous frequencies) were identified in [Casne]. Building on this, all stationary points of the one-dimensional nearest-neighbor XY model (i.e., the Kuramoto model with local coupling) for any given N with either periodic or anti-periodic boundary conditions have been found [Meh09a; MK11; Sme07; Sme08].

Using these solutions, a class of stationary points of the 2-dimensional nearest-neighbor XY model [Ner13] and the XY model with long-range interactions [Kas11] were built and analyzed (see also [Hug13; MS14]). In [Meh09a; MK11; Meh09b; Hug13], all of

the stationary points for small lattices were found using algebraic geometry methods. Bounds on the number of equilibria [BB82] as well as some counterintuitive examples to plausible conjectures [Ara81] have been reported for the same model in the domain of power systems. In [Casne] for the finite N mean-field XY model, and in [Meh09a; Ner13] for the nearest-neighbor XY models, it was shown that there were exponentially many isolated stationary solutions as N increases.

4.2.2 Algebraic geometry interpretation

We initiate an approach to study the Kuramoto model by using an algebraic geometry interpretation of the equilibrium conditions. In Section 4.2.3, we will see how a discriminant locus problem arises.

The equilibrium conditions are $\frac{d\theta_i}{dt} = 0$ for all i. This system of equations has an $O(2)$ freedom, i.e., for any $\alpha \in (-\pi, \pi]$, the equations are invariant under replacing all θ_i with $\theta_i + \alpha$. This rotational symmetry leads to a continua of equilibria. To remove this $O(2)$ freedom and therefore result in only finitely many equilibria, we fix one of the angles, e.g., $\theta_N = 0$, and remove the equation $\frac{d\theta_N}{dt} = 0$ from the system. The remaining system consists of $N-1$ nonlinear equations in $N-1$ angles. Since we assume $\sum_{i=1}^{N} \omega_i = 0$, no information is lost by removing one equation from the system. In [Meh15], we discuss other steps for removing the $O(2)$ freedom.

Upon fixing $\theta_N = 0$ and removing the Nth equation, we have

$$0 = \omega_i - \frac{K}{N} \sum_{j=1}^{N} a_{i,j} \sin(\theta_i - \theta_j)$$

for $i = 1, ..., N-1$. We use the identity

$$\sin(x-y) = \sin x \cos y - \sin y \cos x$$

and substitute $s_i = \sin\theta_i$ and $c_i = \cos\theta_i$ to transform the $N-1$ equations into polynomials that are coupled by the Pythagorean identity $s_i^2 + c_i^2 = 1$. This results in a system of $2(N-1)$ polynomials in $2(N-1)$ variables:

$$\begin{aligned} 0 &= \omega_i + \tfrac{K}{N}\textstyle\sum_{j=1}^{N} a_{i,j}\,(s_i c_j - s_j c_i) \\ 0 &= s_i^2 + c_i^2 - 1 \end{aligned} \tag{4.4}$$

for $i = 1, \ldots, N-1$.

4.2.3 The critical coupling strength K_c

Provided that the coupling strength K is strong enough, the oscillators will synchronize as $t \to \infty$. In particular, a critical coupling K_c exists at which the number of stable equilibria switches from 0 to a nonzero value. Given a network size N, natural frequency vector Ω, and coupling network A, the critical coupling strength K_c is precisely a point on the discriminant locus of system (4.4). Our goal is to compute K_c using numerical algebraic geometry. We will begin by introducing a straightforward algorithm for computing upper and lower bounds on K_c.

In the special case of $N \to \infty$ and long-range (all-to-all) coupling $a_{i,j} = 1$, one may analytically compute K_c. In particular, in [Str00] it is shown that $K_c = 2/(\pi g(0))$ when the ω_i's are chosen according to a unimodal probability density $g(\omega)$ symmetric about a mean of zero. However, for the finite size Kuramoto model, such an analysis may turn out to be very difficult. In particular, finding all equilibria, analyzing stability, and computing

K_c is known to be prohibitively difficult for a finite but large oscillator population.

We will consider $N = 3, \ldots, 18$, and we may denote the critical coupling strength as $K_c(N)$ to emphasize that it is a function of the network size. Different graphs A will be studied, but we will fix the natural frequencies $\Omega = (\omega_1, \ldots, \omega_N)$ to be N equidistant numbers according to $\omega_i = -1 + (2i - 1)/N$. In the case of $N \to \infty$ this corresponds to natural frequencies uniformly distributed on $[-1, 1]$ and it is known that $K_c = 4/\pi$. We will study the finite case with these frequencies, and it is straightforward to generalize our method to other distributions.

In [VM09; VM08; DB11], necessary and sufficient conditions are given for fixed points to exist for the finite size Kuramoto model for complete and bipartite graphs, and explicit upper and lower bounds of $K_c(N)$ for these systems were also computed, followed by providing an algorithm to compute $K_c(N)$. For the complete graph, similar results were presented in [AR04; MS05], where it was additionally shown that there is exactly one single stable equilibrium for $K > K_c(N)$. In [Dör13], an analogous result was shown for acyclic graphs, short cycles, and complete graphs as well as combinations thereof. In the case of homogeneous natural frequencies networks with sufficiently high nodal degrees, the only stable fixed point is known to be the phase-synchronized solution [Tay12]. In [OG09], all of the stable synchronized states were classified for the one-dimensional Kuramoto model on a ring graph with random natural frequencies in addition to computing a lower bound on $K_c(N)$ (see also [Erm85; SM88]).

Our algebraic geometry interpretation of the Kuramoto model immediately yields the following algorithm for numerically computing upper and lower bounds on $K_c(N)$ given fixed $\Omega = (\omega_1, \ldots, \omega_{N-1})$ and $A = [a_{ij}]$. First, we begin with known or estimated bounds B_ℓ and B_u. Using parameter homotopies as outlined in Section 2.4.4, we compute all solutions to polynomial system (4.4) at many K values in the interval

$[B_\ell, B_u]$. For each K value tested, we discard nonreal solutions. For each real solution $(s_1, \ldots, s_{N-1}, c_1, \ldots, c_{N-1})$, we compute the corresponding angles $(\theta_1, \ldots, \theta_N)$ and compute the eigenvalues of the Jacobian of (4.2) evaluated at $(\theta_1, \ldots, \theta_N)$. The *index* of the solution is the number of positive eigenvalues, and real solutions with index zero correspond to stable steady states. The maximum value of K tested such that no stable solutions exist is a lower bound on K_c, and the minimum value of K tested such that stable solutions exist is an upper bound on K_c.

4.2.4 Results for the complete graph

We start with the most prominent and well studied case, which is the complete graph, namely $a_{i,j} = 1$ for all i, j. We perform the algorithm of Section 4.2.3 for $N = 3, \ldots, 18$ with $[B_\ell, B_u] = [1, 2]$. Figure 4.1 summarizes the number of real-valued solutions to the polynomial system (4.4).

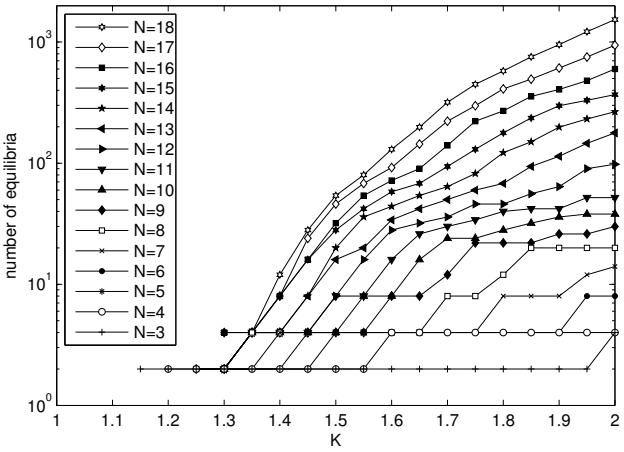

Figure 4.1: Number of equilibria for the case of equidistant natural frequencies on the complete graph at $1 \leq K \leq 2$.

Once the real solutions are found, we turn our attention to determining which ones are stable. Via Jacobian analysis we find that there is exactly one stable steady state solution for $N = 3, \ldots, 18$ at each K value tested, with the exception of small values of K which result in no real solutions. This result is consistent with theoretic findings for the complete graph [AR04; MS05; DB11; VM08]. Next, for each N we use the results of our stability analysis to determine numerical upper and lower bounds on $K_c(N)$. These results are presented in Figure 4.2. We verify that these bounds for $K_c(N)$ are consistent with the known explicit bounds from Corollary 6.7 of [DB14]. For $N \in \{3, 4\}$, our computed lower bound is less than the explicit lower bound due to the coarse resolution of tested numeric values for $K_c(N)$.

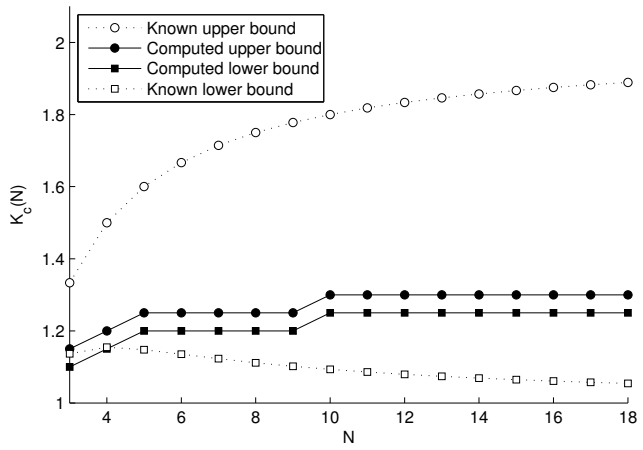

Figure 4.2: Bounds for $K_c(N)$ in the case of equidistant natural frequencies on the complete graph. Known explicit bounds from Corollary 6.7 of [DB14] are shown for comparison.

As mentioned earlier, our stability analysis is based on computing the index corresponding to each real solution. Figure 4.3 shows a histogram of these values for the

case $K = 100$. In this case, we use a large coupling strength to demonstrate a greater number of equilibria. We observe that when j is small enough relative to N, the number

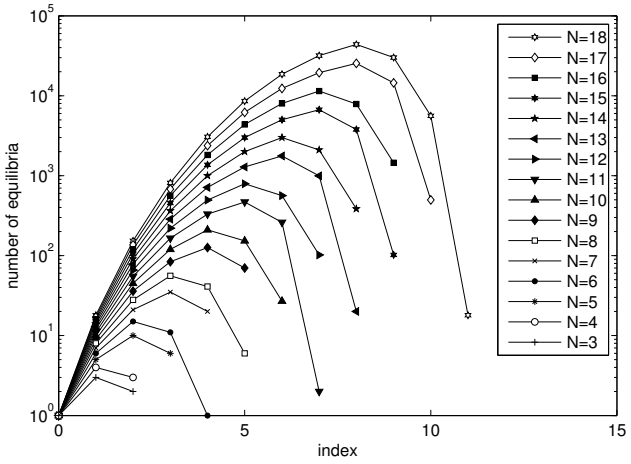

Figure 4.3: Number of equilibria with given index for equidistant natural frequencies and a complete graph with $K = 100$.

of real solutions with index j is exactly $\binom{N}{j}$. In particular, for $3 \leq N \leq 4$ this behavior occurs for $j \leq 1$ and, for $5 \leq N \leq 18$, this behavior occurs for $j \leq \lceil \frac{2}{5}(N-1) \rceil$. Based on these results, we conjecture that this phenomenon occurs in general: for equidistant natural frequencies, if $0 \leq j \ll N$ and $K \gg 0$, then the number of equilibria with index j is expected to be $\binom{N}{j}$. This conjecture can be used when N may be too large to compute all solutions. For example, we expect 75,287,520 real equilibria of index 5 for $N = 100$.

4.2.5 Results for cyclic graphs

Although our investigation initially focused on the complete graph being the most well studied case, we also performed a preliminary analysis of the coupling arrangement defined

by an undirected cyclic graph. Cyclic graphs are known for having multi-stable equilibria [DB14] and entirely unstable equilibrium landscapes [Ara81], and therefore exhibit quite distinct behavior from acyclic or complete graphs [Dör13; Wil06; Erm85].

For $N = 10$, we used the same equidistant natural frequencies mentioned earlier with Figure 4.4 showing the number of equilibria and the number of stable equilibria at each integer $K = 0, \ldots, 100$. For some values of K, the system possesses only unstable equilibria.

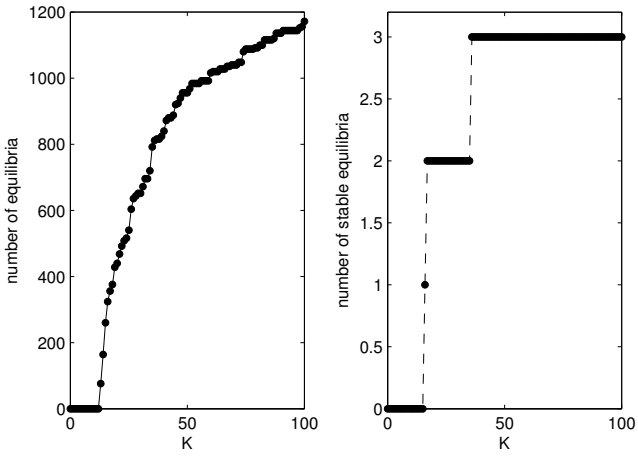

Figure 4.4: Number of equilibria and number of stable equilibria for a cyclic coupling arrangement when $N = 10$.

In particular, when K is 13, 14, or 15, there are 76, 164, and 260 equilibria, respectively, all of which are unstable. Since the critical points of the potential (4.3) correspond to power flow in a transmission network, an interesting technological implication of these results is that there are power demands which can be met only with unstable equilibria. We find one stable equilibria at $K = 16$ and conclude $15 \leq K_c(10) \leq 16$. Figure 4.4 also indicates multistability for some values of K, with at most *three* stable equilibria for each investigated sample. These results are in contrast to the complete graph case, in which

exactly one stable equilibria exists whenever the system has real-valued solutions.

Next, we take a closer look at the geometric configuration of angles occurring at the stable equilibria shown in Figure 4.4. For relatively small K such as $K = 16, 17, 18$, the configuration of angles at stable equilibria shows no discernible structure. For $K = 35$ there are two stable equilibria, with one exhibiting phase sync, i.e., angles clustered around 0, and one exhibiting a splay state, i.e., angles approximately uniformly distributed on $[0, 2\pi)$. For the splay state, the θ_i decrease on $[0, 2\pi)$.

For each $K = 36, \ldots, 100$ there are three stable equilibria, with each case consisting of one phase sync and two splay states. In one of these splay states $\theta_1, \ldots, \theta_9$ are arranged in increasing order on $[0, 2\pi)$, and in the other $\theta_9, \ldots, \theta_1$ are arranged in decreasing order on $[0, 2\pi)$. In Figure 4.5, we depict the three stable equilibria at $K = 100$. As K increases, the steady state phase sync gradually becomes more tightly clustered, with the angle range decreasing from ~ 0.9432 for $K = 35$ to ~ 0.3256 for $K = 100$. This is in accordance with the asymptotic result that exact phase sync is a critical point of the Kuramoto potential (4.3) as $K \to \infty$ [DB14].

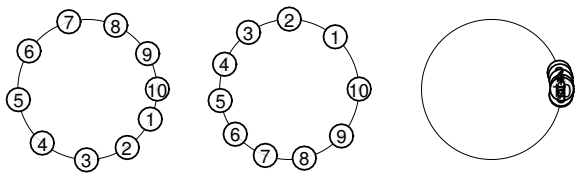

Figure 4.5: Configuration of $\theta_1, \ldots, \theta_{10}$ for the three stable equilibria occurring at $K = 100$ for a cyclic graph with $N = 10$.

4.2.6 Results for random graphs

We now turn our attention to random coupling arrangements. In these computations, we choose each $a_{i,j}$ as 0 or 1 according to a pre-determined probability P while setting $a_{j,i} = a_{i,j}$. In other words, $[a_{i,j}]$ is the adjacency matrix of a symmetric Erdös-Rényi random graph with coupling probability P, where we restrict our attention to undirected, connected graphs. For these numerical experiments, we use the same equidistant natural frequencies discussed earlier.

We fix $N = 10$ and investigate how $K_c(N)$ depends on the density of the graph. For each coupling probability $P = 0.25, 0.375, \ldots, 0.875$, we generated 100 random graphs. For each graph, we computed equilibria and determine stability at the following values of K: for $P = 0.25$ we use $K = 1, \ldots, 20$; for $P = 0.375$ we use $K = 1, \ldots, 15$; for $P = 0.5$ we use $K = 1, \ldots, 10$; and for each $P = 0.625, 0.75, 0.875$, we use $K = 1, \ldots, 5$. In all cases, we find a value of K such that at least one stable equilibrium occurs at K while no stable equilibria occur at $K - 1$, thereby allowing us to estimate bounds on $K_c(10)$. Figure 4.6 shows these results sorted according to the number of cycles in the graph.

For undirected and connected graphs, a theoretic lower bound and a conjectured theoretic upper bound are [DB14; Dör13]

$$N \cdot \max_i \left\{ \frac{|\omega_i|}{\deg_i} \right\} \leq K_c(N) \leq N \cdot \|B^T L^\dagger \omega\|_\infty,$$

where $\deg_i = \sum_j a_{ij}$ is the degree of node i, B is the oriented incidence matrix, and L is the network Laplacian matrix. These bounds are shown in Figure 4.6 for comparison. We verified that our 600 individual results as well as the averages shown are consistent with these theoretic bounds and validate their accuracy. Figure 4.6 indicates that the numerical

upper bound is tighter than the theoretic bound on average, while the numerical lower bound tends to be weaker. Since the tightness of our computed bounds depends on the resolution of K values tested, one could check more refined K values to obtain tighter numerical bounds for particular graphs of interest.

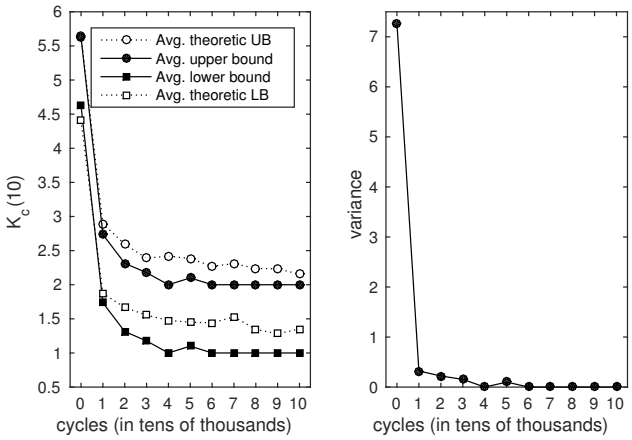

Figure 4.6: Average bounds on $K_c(N)$ for random graphs according to number of cycles in the case of $N = 10$.

4.2.7 Further progress towards K_c

In our discussion of the Kuramoto model thus far, we have not fully utilized the fact that K_c is a point on a discriminant locus. In this subsection, we present recent progress towards a more precise method of computing K_c.

Fix $\Omega = (\omega_1, \ldots, \omega_N)$ and $A = [a_{ij}]$. Let $G(\theta; K) = 0$ denote the polynomial system

(4.4), where $\theta = (\theta_1, \ldots, \theta_N)$. The critical point $K = K_c$ is a solution to

$$F(\theta; K) = \begin{bmatrix} G(\theta; K) \\ \det J_\theta G(\theta; K) \end{bmatrix} = 0 \tag{4.5}$$

for some $\theta \in \mathbb{R}^N$, where we write $J_\theta G$ to indicate that the Jacobian is taken with respect to θ only. One approach to find K_c would be to use system (4.5) directly. However, this would require computing $\det J_\theta G(\theta; K)$, which quickly becomes difficult as N increases.

Rather than work directly with $\det J_\theta G(\theta; K)$, we can instead construct a homotopy to force the system to become rank deficient. In this way, we obtain the desired solution $(\theta; K_c)$ to system (4.5) without having a symbolic expression for the determinant.

First, let $\alpha, \beta \in \mathbb{C}^{2(N-1)}$ be random nonzero vectors, and let $\gamma = \alpha \cdot \beta$. Let $v^* = \beta/\gamma$ so that $\alpha \cdot v^* = 1$. Next, we choose a value $K^* \in \mathbb{R}$ that is known to be larger than K_c but such that $K^* - K_c$ is small. We fix a time step Δt and run iterations of the Kuramoto model as a dynamical system, where $K = K^*$ with random starting phases θ_i. At each step, we check the rate of change of each θ_i. After a sufficient number of iterations, we find every θ_i has a rate of change below some pre-defined threshold, indicating that $\frac{d\theta_i}{dt}$ is numerically zero. We let θ^* denote the angles of this equilibrium.

Next, we use $(\theta, v, K; t) = (\theta^*, v^*, K^*; 1)$ as a starting point in the following homotopy:

$$H(\theta, v, K; t) = \begin{bmatrix} G(\theta; K) \\ J_\theta G(\theta; K) \cdot v - t \cdot J_\theta G(\theta^*; K^*) \cdot v^* \\ \alpha \cdot v - 1 \end{bmatrix} = 0. \tag{4.6}$$

We track $t \in \mathbb{R}$ from 1 to 0. At $t = 0$ we have $J_\theta G(\theta; K) \cdot v = 0$ while $v \neq 0$, and therefore system (4.5) is satisfied. We arrive at a value of K on the discriminant locus, which is a

finite set of points. Provided that we began with a sufficiently close initial guess K^*, the endpoint of homotopy (4.6) is $(\theta, v, K; t) = (\theta, v, K_c; 0)$ for some θ and v.

In Figure 4.7 we summarize our results for this method in the case of the complete graph with equidistant natural frequencies. For comparison, we also show the bounds that were presented earlier in Figure 4.2. In Figure 4.8, we show zoomed in regions to illustrate that the new results are within our numerical bounds.

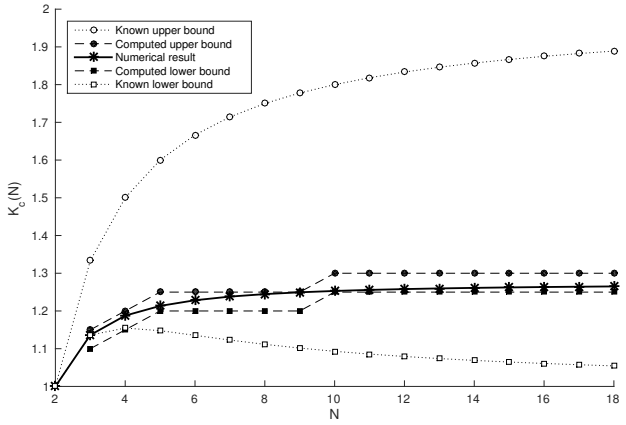

Figure 4.7: $K_c(N)$ for the complete graph with equidistant natural frequencies.

Performing this algorithm with numerical homotopy tracking in `Bertini` allows us to compute K_c to an arbitrary precision. For example, the first 80 digits of $K_c(4)$ are

1.18766435188606583602297825019273584400694074887815146225064778326462155080353 77.

Since we know K_c is algebraic, computing its value to a high precision is useful for finding its minimal polynomial. Using these high precision expressions for K_c with Maple's `MinimalPolynomial` command, we find the following results to be true to at least 1000 digits.

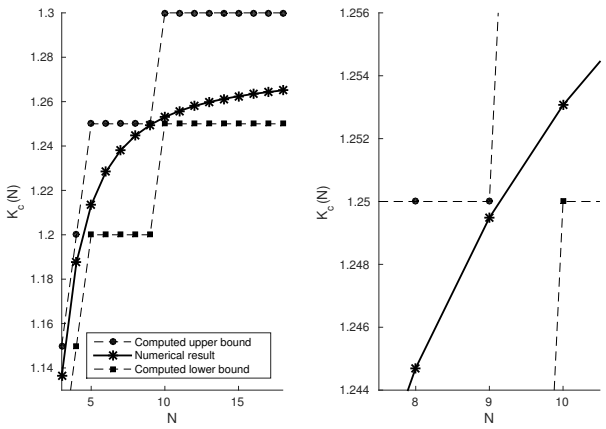

Figure 4.8: Zoomed regions from Figure 4.7.

Proposition 4.2.1 *For the complete graph with equidistant natural frequencies as described above, the following hold.*

1. $K_c(3)$ *is a root of*

$$1024 - 828x^2 + 27x^4.$$

Specifically,

$$K_c(3) = \frac{1}{3}\sqrt{2(69 - 11\sqrt{33})}.$$

2. $K_c(4)$ *is a root of*

$$-81 - 2380x^2 + 1728x^4.$$

Specifically,

$$K_c(4) = \frac{1}{12}\sqrt{\frac{1}{6}(595 + 73\sqrt{73})}.$$

3. $K_c(5)$ *is a root of*

$$-603979776 - 2267545600x^2 - 2583168000x^4 + 3785280000x^6$$
$$-536930000x^8 - 2475000x^{10} + 84375x^{12}.$$

4. $K_c(6)$ *is a root of*

$$-2562890625 - 645012112500x^2 - 8952920813214x^4$$
$$+1647652604060x^6 - 7193942886921x^8 + 6402589992960x^{10}$$
$$+333734078464x^{12} - 60280012800x^{14} + 1387266048x^{16}.$$

4.3 An application to lattice field theory

4.3.1 Statement of the problem

In theoretical physics, quantum field theory (QFT) provides a foundation for quantum mechanical models. Although fields in physics are continuous, lattice field theories use a discretized view of spacetime. Treating spacetime as a lattice facilitates computations which may provide valuable insight into QFT. Such formulations often make use of a function known as a gauge-fixing partition function, denoted Z_{GF}. In recent years, a theory has been proposed for the stereographic lattice Landau gauge [Sme07; Sme08; Meh09a]. To test the validity of this theory, we are interested in determining whether or not it yields a valid function Z_{GF} when working on the 3×3 lattice. The work that follows can be found in [Meh14], which includes more technical details regarding the physics involved. The problem and its formulation are based on [Meh09a].

In this setting, Z_{GF} counts the number of real stationary points for a system of ODEs. As we did in Section 4.2, we convert the stationary point conditions into a system of polynomials depending on parameters. For the proposed theory to be valid, Z_{GF} must be orbit independent, meaning that all choices of parameters must result in the same number of real solutions. We find that randomly choosing parameter values leads to the same number of real solutions each time. Our goal is to determine whether or not a discriminant locus exists for which nongeneric behavior occurs in the number of real solutions. Using numerical algebraic geometry, we will see that such parameter choices do exist, and hence the proposed theory is not a valid topological field theory. These parameter values form a discriminant locus which we investigate numerically.

Let $\mathbf{j} = (j_1, j_2)$ denote a position on the two-dimensional lattice. The variables of the system are angles at each lattice site, which we denote $\theta_{\mathbf{j}}$. We use μ to denote a directional index, which indicates movement along one of the two dimensions of the lattice. In practice, we use $\mu = 1$ to denote "move one unit to the left" and $\mu = 2$ to denote "move one unit up". We let $\hat{\mu}$ denote the opposite direction of μ, and $\mathbf{j} + \mu$ or $\mathbf{j} + \hat{\mu}$ indicates the position on the lattice that is one unit from $\mathbf{j}$ in the indicated direction. The model has 18 parameters $\phi_{\mathbf{j},\mu}$, and we let $\phi^{\theta}_{\mathbf{j},\mu} = \phi_{\mathbf{j},\mu} + \theta_{\mathbf{j}+\hat{\mu}} - \theta_{\mathbf{j}}$. In this setting, the system of equations we are interested in is

$$0 = \sum_{\mu} \Big(\tan(\phi^{\theta}_{\mathbf{j},\mu}/2) - \tan(\phi^{\theta}_{\mathbf{j}-\hat{\mu},\mu}/2) \Big) \tag{4.7}$$

for each $\mathbf{j} = (1,1), \ldots, (3,3)$.

As we did in Section 4.2, we fix $\theta_{3,3} = 0$ and remove the last equation to ensure that there are only isolated solutions. Next, we will transform our system of trigonometric equations into a system of polynomial equations. Our first step is to expand (4.7) and

use the trigonometric identity

$$\tan\frac{x+y+z}{2}=\frac{\sin x+\cos z\sin y+\cos y\sin z}{\cos x+\cos y\cos z-\sin y\sin z}.$$

This yields equations of the form

$$\begin{aligned}0 &= \sum_{\mu}\Big(\frac{\sin\phi_{\mathbf{j},\mu}\cos\theta_{\mathbf{j}}-\cos\phi_{\mathbf{j},\mu}\sin\theta_{\mathbf{j}}+\sin\theta_{\mathbf{j}+\hat{\mu}}}{\sin\phi_{\mathbf{j},\mu}\sin\theta_{\mathbf{j}}+\cos\phi_{\mathbf{j},\mu}\cos\theta_{\mathbf{j}}+\cos\theta_{\mathbf{j}+\hat{\mu}}}\\ &\quad -\frac{\sin\phi_{\mathbf{j}-\hat{\mu},\mu}\cos\theta_{\mathbf{j}-\hat{\mu}}-\cos\phi_{\mathbf{j}-\hat{\mu},\mu}s_{\mathbf{j}-\hat{\mu}}+\sin\theta_{\mathbf{j}}}{\sin\phi_{\mathbf{j}-\hat{\mu},\mu}\sin\theta_{\mathbf{j}-\hat{\mu}}+\cos\phi_{\mathbf{j}-\hat{\mu},\mu}\cos\theta_{\mathbf{j}-\hat{\mu}}+\cos\theta_{\mathbf{j}}}\Big).\end{aligned}$$

We then remove the trigonometric conditions by letting $s_{\mathbf{j}}=\sin\theta_{\mathbf{j}}$ and $c_{\mathbf{j}}=\cos\theta_{\mathbf{j}}$ for all $\mathbf{j}$ and introducing the equations $s_{\mathbf{j}}^2+c_{\mathbf{j}}^2-1=0$. Then, for all $\mathbf{j}$ except $(3,3)$ we have

$$\begin{aligned}0 &= \sum_{\mu}\Big(\frac{\sin\phi_{\mathbf{j},\mu}c_{\mathbf{j}}-\cos\phi_{\mathbf{j},\mu}s_{\mathbf{j}}+s_{\mathbf{j}+\hat{\mu}}}{\sin\phi_{\mathbf{j},\mu}s_{\mathbf{j}}+\cos\phi_{\mathbf{j},\mu}c_{\mathbf{j}}+c_{\mathbf{j}+\hat{\mu}}}\\ &\quad -\frac{\sin\phi_{\mathbf{j}-\hat{\mu},\mu}c_{\mathbf{j}-\hat{\mu}}-\cos\phi_{\mathbf{j}-\hat{\mu},\mu}s_{\mathbf{j}-\hat{\mu}}+s_{\mathbf{j}}}{\sin\phi_{\mathbf{j}-\hat{\mu},\mu}s_{\mathbf{j}-\hat{\mu}}+\cos\phi_{\mathbf{j}-\hat{\mu},\mu}c_{\mathbf{j}-\hat{\mu}}+c_{\mathbf{j}}}\Big)\\ 0 &= s_{\mathbf{j}}^2+c_{\mathbf{j}}^2-1.\end{aligned}\tag{4.8}$$

Next, we introduce auxiliary variables $a_{\mathbf{j},\mu},b_{\mathbf{j},\mu}$ in place of denominators along with the appropriate polynomial conditions to satisfy the system. The resulting polynomial

system is:

$$\begin{aligned}
0 &= \sum_{\mu} \Big(a_{\mathbf{j},\mu}(\sin\phi_{\mathbf{j},\mu} c_{\mathbf{j}} - \cos\phi_{\mathbf{j},\mu} s_{\mathbf{j}} + s_{\mathbf{j}+\hat{\mu}}) \\
&\quad - b_{\mathbf{j},\mu}(\sin\phi_{\mathbf{j}-\hat{\mu},\mu} c_{\mathbf{j}-\hat{\mu}} - \cos\phi_{\mathbf{j}-\hat{\mu},\mu} s_{\mathbf{j}-\hat{\mu}} + s_{\mathbf{j}}) \Big) \\
0 &= a_{\mathbf{j},\mu}(\sin\phi_{\mathbf{j},\mu} s_{\mathbf{j}} + \cos\phi_{\mathbf{j},\mu} c_{\mathbf{j}} + c_{\mathbf{j}+\hat{\mu}}) - 1 \\
0 &= b_{\mathbf{j},\mu}(\sin\phi_{\mathbf{j}-\hat{\mu},\mu} s_{\mathbf{j}-\hat{\mu}} + \cos\phi_{\mathbf{j}-\hat{\mu},\mu} c_{\mathbf{j}-\hat{\mu}} + c_{\mathbf{j}}) - 1 \\
0 &= s_{\mathbf{j}}^2 + c_{\mathbf{j}}^2 - 1. \qquad (4.9)
\end{aligned}$$

We now have 48 polynomial equations in 48 variables. Although this system is larger than system (4.7), the key benefit of this polynomial formulation is that it enables us to use numerical algebraic geometry. We note that this is a one-to-one transformation and no solutions of the original system are lost in the transformation.

4.3.2 Methods and results

To determine the behavior of the system at general points in the parameter space, we use parameter homotopies to sove the system for 780 random sets of parameters $\{\phi_{\mathbf{j},\mu}\}$. In each instance, we find that there are 11664 real solutions. As a result, we conjecture that for all points in the parameter space except a set of measure zero, the system has exactly 11664 real solutions.

Next, we investigate the measure zero discriminant locus on which the system has nongeneric behavior. We find that when the angles in $\{\phi_{\mathbf{j},\mu}\}$ are deliberately chosen so that they adhere to some structure, such as rational multiples of π, it is quite easy to find a point in the parameter space such that the system has fewer than 11664 real solutions. Thus, the number of stationary points differs for various orbits, and Z_{GF} for

the stereographic lattice Landau gauge-fixing functional is orbit-dependent. We conclude that the proposed theory is not a valid topological field theory.

We summarize our results in the following figures. In Figure 4.9, we plot the number of real solutions corresponding to various sets of parameters $P_1, \ldots, P_4$. In Figure 4.10, we plot a subset of the discriminant locus projected onto the two parameters $\phi_{(1,1),1}$ and $\phi_{(1,1),2}$ in which the rest of the parameters are fixed to the angles given in Table 4.1. To locate points on the discriminant locus, we used the fact that for parameter values to result in fewer than 11664 real solutions, we must have denominator(s) equal to zero in system (4.8). Since we introduced auxiliary variables for denominators when constructing the polynomial system, we can perform parameter homotopies in which the destination systems have one or more of these 'denominators' equal to zero. We note that the points shown here are only a subset of the discriminant locus, which is an algebraic curve in this projection. Nevertheless, these computed points illustrate the abundance of parameter choices for which the system has nongeneric behavior.

Table 4.1: Fixed parameter values used for Figure 4.10.

j_1	1	1	2	2	2	3	3	3
j_2	2	3	1	2	3	1	2	3
μ	1	1	1	1	1	1	1	1
$\phi_{(j_1,j_2),\mu}$	$-\frac{\pi}{2}$	$\frac{\pi}{5}$	$-\frac{5\pi}{11}$	$\frac{15\pi}{17}$	$-\frac{15\pi}{23}$	$\frac{28\pi}{31}$	$\frac{24\pi}{41}$	$-\frac{7\pi}{47}$

j_1	1	1	2	2	2	3	3	3
j_2	2	3	1	2	3	1	2	3
μ	2	2	2	2	2	2	2	2
$\phi_{(j_1,j_2),\mu}$	$\frac{2\pi}{3}$	$-\frac{5\pi}{7}$	$\frac{\pi}{13}$	$\frac{17\pi}{19}$	$\frac{27\pi}{29}$	$-\frac{\pi}{37}$	$-\frac{30\pi}{43}$	$\frac{44\pi}{53}$

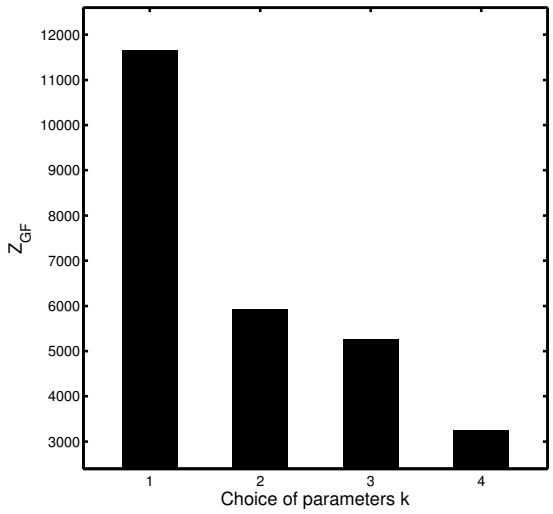

Figure 4.9: Z_{GF} corresponding to various sets of parameters P_k which are defined as follows. For P_1, we set each parameter to a distinct angle via $\phi_{j_1,j_2,\mu} = \pi/(j_2 + 3(j_1 - 1) + 9(\mu - 1))$. For P_2, we set $\phi_{\mathbf{j},\mu} = \pi/2$ for all $\mathbf{j}$ and μ. For P_3, we set $\phi_{\mathbf{j},\mu} = 0$ for all $\mathbf{j}$ and μ. For P_4, we set $\phi_{\mathbf{j},\mu} = \pi/3 + (\pi/6)(\mu - 1)$.

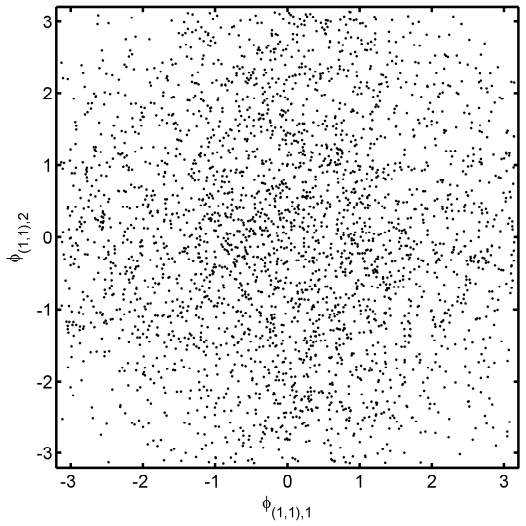

Figure 4.10: Subset of the discriminant locus projected onto two parameters for the 3×3 lattice.

Chapter 5

Secant varieties and tensor rank

5.1 Introduction

Let $X \subset \mathbb{P}^n$ be an irreducible, projective algebraic set. The *X-rank* of an element $T \in \mathbb{P}^n$, denoted $\mathrm{rk}_X(T)$, is the minimum $r \in \mathbb{N}$ such that T can be written as a sum of r elements of X:

$$T = \sum_{i=1}^{r} x_i, \quad x_i \in X.$$

Let $\sigma_r^0(X) \subset \mathbb{P}^n$ denote the set of elements with rank at most r. The *kth secant variety* of X is

$$\sigma_k(X) = \overline{\sigma_k^0(X)}.$$

If $T \in \sigma_r(X)$, then T is the limit of a sequence of elements of X-rank at most r. The *X-border rank* of an element $T \in \mathbb{P}^n$, denoted $\mathrm{brk}_X(T)$, is the minimum $r \in \mathbb{N}$ such that $T \in \sigma_r(X)$. From these definitions, we naturally have

$$\mathrm{brk}_X(T) \leq \mathrm{rk}_X(T)$$

for any $T \in \mathbb{P}^n$ and $X \in \mathbb{P}^n$. When X is clear from context, we may simply write $\mathrm{brk}(T)$ and $\mathrm{rk}(T)$ instead of $\mathrm{brk}_X(T)$ and $\mathrm{rk}_X(T)$.

Secant varieties are classical objects in algebraic geometry, and there has been a renewed interest in them in recent years due to applications of tensor decomposition. Tensor decomposition plays a fundamental role in areas including computational complexity, signal processing for telecommunications [DLC07], [Com02], scientific data analysis [Smi05], [JS04], electrical engineering [Che05], and statistics [McC87]. Some other applications include the complexity of matrix multiplication [Str83], the complexity problem of P versus NP [Val01], the study of entanglement in quantum physics [EG05], matchgates in computer science [Val01], the study of phylogenetic invariants [AR08], independent component analysis [Com92], blind identification in signal processing [Sid00], branching structure in diffusion images [SS08], and other multilinear data analytic techniques in bioinformatics and spectroscopy [CJ10].

From the definitions above, secant varieties can be written as the closure of a polynomial image of an algebraic set. In principle, one can test whether or not an element T belongs to a given kth secant variety (and hence whether $\mathrm{brk}_X(T) \leq k$) via the defining equations of the variety. However, these defining equations are often of high degree, making it difficult or impractical to compute them using symbolic elimination theory. This secant varieties natural targets for algorithms in numerical elimination theory.

5.2 Determining tensor rank

In this section, we work with secant varieties $\sigma_k(X)$ where X is a Veronese variety which arises in the following setting.

Fix $n \in \mathbb{N}$ and let $S = \mathbb{C}[x_0, \ldots, x_n]$. Then

$$S^d V = \left\langle x_0^d, x_1^{d-1} x_1, \ldots, x_n^d \right\rangle.$$

That is, $S^d V$ is the vector space of homogeneous forms in $n+1$ variables of degree d. Or, equivalently, $S^d V$ is the space of symmetric tensors of order d over a vector space of dimension $n+1$.

Finding the minimum $r \in \mathbb{N}$ such that $T \in S^d V$ is equivalent to computing the X-rank where X is the Veronese variety $X = \nu_d(\mathbb{P}^n)$. We can view the problem of decomposing a symmetric tensor as

$$T = \sum_{i=1}^{r} v_i^{\otimes d}$$

where $v_i \in V$, or equivalently as decomposing the corresponding homogeneous polynomial

$$T = \sum_{i=1}^{r} L_i^d \tag{5.1}$$

where each L_i is a linear form.

We utilize the fact that $\sigma_k^0(X)$ can be written as a polynomial image of an algebraic set. The closure of the image, $\sigma_k(X) = \overline{\sigma_k^0(X)}$, is the set of elements with border rank less than or equal to k. Thus if $T \in \sigma_k(X)$ we can conclude $\operatorname{brk}(T) \leq k$, and if $T \notin \sigma_k(X)$ we can conclude $\operatorname{brk}(T) > k$. Although these membership tests can be performed symbolically, difficulties may arise in practice due to the degree of X. In these cases, we may be able to compute a pseudowitness set and use it for numerical membership testing.

The X-rank and the X-border rank of monomials with respect to the Veronese variety

are well known over the complex numbers ([RS11], [Boi11]): if $T = x_1^{\alpha_1} \cdots x_n^{\alpha_n}$, then

$$\operatorname{brk}(T) = \frac{\Pi_{i_1}^n(\alpha_i + 1)}{\max_i(\alpha_i + 1)}$$

and

$$\operatorname{rk}(T) = \frac{\Pi_{i_1}^n(\alpha_i + 1)}{\min_i(\alpha_i + 1)}.$$

For other homogeneous polynomials, there are a multitude of open problems.

We will proceed using a numerical membership test from [HS13] adapted to our current problem. For each $r \geq 1$, consider the smooth irreducible variety

$$X_r = \left\{ (S, L_1, \ldots, L_r) \;\middle|\; S = \sum_{i=1}^{r} L_i^d \right\} \subset S^d V \times \underbrace{S^1 V \times \cdots \times S^1 V}_{r \text{ times}}. \tag{5.2}$$

which has dimension $r \cdot \dim V$. For the projection map $\pi(S, L_1, \ldots, L_r) = S$, we have

$$\pi(X_r) = \sigma_r^0(\nu_d(V)) \quad \text{and} \quad \overline{\pi(X_r)} = \sigma_r(\nu_d(V)).$$

The key to the membership test of [HS13] is to perform all numerical computations on X_r for which defining equations are known, namely $X_r = V(F_r)$ where

$$F_r(S, L_1, \ldots, L_r) = S - p_d(L_1, \ldots, L_r) \text{ where } p_d(L_1, \ldots, L_r) = \sum_{i=1}^{r} L_i^d.$$

One way to compute the dimension of $\sigma_r(\nu_d(V))$ is by using Lemma 3 of [HS13] which, in this case, states that

$$\dim \sigma_r(\nu_d(V)) = \dim X_r - \dim \operatorname{null} Jp_d(L_1^*, \ldots, L_r^*)$$

for generic $L_i^* \in S^1V$ where Jp_d is the Jacobian matrix of p_d.

The membership test provided in [HS13] is based on the standard homotopy membership test described in [Bat13] using pseudowitness sets. Let $T \in S^dV$ be given and suppose that $m = \dim \sigma_r(\nu_d(V))$ and $k = \dim X_r - m$. For $i = 1, \ldots, m$, let $M_i(S)$ and $R_i(S)$ be general linear forms such that $R_i(T) = 0$. That is, $\mathcal{M} = \mathcal{V}(M_1, \ldots, M_m)$ and $R = \mathcal{V}(R_1, \ldots, R_m)$ are general codimension m linear spaces with $T \in \mathcal{V}(R_1, \ldots, R_m)$. The underlying idea of the homotopy membership test is that, given the finitely many points in $\sigma_r(\nu_d(V)) \cap \mathcal{M}$, we follow the paths starting at each of these points defined by $\sigma_r(\nu_d(V)) \cap (\mathcal{M} \cdot t + \mathcal{R} \cdot (1-t))$ as t moves from 1 to 0. Then, $T \in \sigma_r(\nu_d(V))$ if and only if one of the paths limits to T as $t \to 0$.

This computation is performed on X_r as follows. For $j = 1, \ldots, k$, let $\widehat{M}_j(L_1, \ldots, L_r)$ be general linear forms with $\widehat{\mathcal{M}} = \mathcal{V}(\widehat{M}_1, \ldots, \widehat{M}_k)$. Then, $X_r \cap \mathcal{M} \cap \widehat{\mathcal{M}}$ consists of finitely many points with $|\pi(X_r)\mathcal{M} \cap \widehat{\mathcal{M}}| = \deg \sigma_r(\nu_d(V))$. Let $W \subset X_r \cap \mathcal{M} \cap \widehat{\mathcal{M}}$ be a set of $\deg \sigma_r(\nu_d(V))$ such that $|\pi(W)| = |W|$. For each $w \in W$, consider the path $Z_w(t)$ with

$$Z_w(1) = w \quad \text{and} \quad Z_w(t) \in X_r \cap (\mathcal{M} \cdot t + \mathcal{R} \cdot (1-t)) \cap \widehat{\mathcal{M}}.$$

With this setup, we have the following basic membership test of Lemma 1 from [HS13].

Proposition 5.2.1 *For the setup described above, the following hold.*

1. $T \in \sigma_r(\nu_d(V))$ *if and only if there exists* $w \in W$ *such that* $\lim_{t\to 0} \pi(Z_w(t)) = T$.

2. $T \in \sigma_r^0(\nu_d(V))$ *if there exists* $w \in W$ *such that* $\lim_{t\to 0} Z_w(t) \in X_r$ *and* $\lim_{t\to 0} \pi(Z_w(t)) = T$.

3. *If, for every* $w \in W$, $\lim_{t\to 0} Z_w(t) \in X_r$, *then,* $T \in \sigma_r^0(\nu_d(V))$ *if and only if there exists* $w \in W$ *such that* $\lim_{t\to 0} \pi(Z_w(t)) = T$.

We demonstrate our method with the following examples. Further applications are explored in [Ber15].

Example 5.2.2 *Consider the X-border rank over the complex numbers with respect to the Veronese variety $\nu_5(\mathbb{P}^2)$ of*

$$T = x^3y^2 + x^4z.$$

T is the sum of two monomials with x appearing in both, and therefore it is not covered by [Car12]. We begin by testing for border rank 4, which requires computing a pseudowitness set for $\sigma_4(\nu_5(\mathbb{P}^2))$.

Tensors in $\sigma_4(\nu_5(\mathbb{P}^2))$ correspond to degree 5 homogeneous polynomials in 3 variables with degree less than or equal to 4, so we consider the expression

$$\sum_{i=1}^{4}(a_{i,1}x + a_{i,2}y + a_{i,3}z)^5.$$

There are $\binom{5+3-1}{3} = 21$ monomials of degree 5 in 3 variables, and expanding the above allows us to write these monomials with coefficients in $a_{i,j}$. For example, the coefficient of x^3y^2 in the above expression is $10a_{11}^3a_{12}^2 + 10a_{21}^3a_{22}^2 + 10a_{31}^3a_{32}^2 + 10a_{41}^3a_{42}^2$.

Altogether, our object of interest is the closure of the image of the polynomial map $p : \mathbb{C}^{12} \to \mathbb{C}^{21}$ defined by:

$$
\begin{aligned}
p_1 &= 20a_{11}a_{12}a_{13}^3 + 20a_{21}a_{22}a_{23}^3 + 20a_{31}a_{32}a_{33}^3 + 20a_{41}a_{42}a_{43}^3 \\
p_2 &= 30a_{11}^2a_{12}a_{13}^2 + 30a_{21}^2a_{22}a_{23}^2 + 30a_{31}^2a_{32}a_{33}^2 + 30a_{41}^2a_{42}a_{43}^2 \\
p_3 &= 30a_{11}^2a_{12}^2a_{13} + 30a_{21}^2a_{22}^2a_{23} + 30a_{31}^2a_{32}^2a_{33} + 30a_{41}^2a_{42}^2a_{43} \\
p_4 &= 20a_{11}a_{12}^3a_{13} + 20a_{21}a_{22}^3a_{23} + 20a_{31}a_{32}^3a_{33} + 20a_{41}a_{42}^3a_{43} \\
p_5 &= 20a_{11}^3a_{12}a_{13} + 20a_{21}^3a_{22}a_{23} + 20a_{31}^3a_{32}a_{33} + 20a_{41}^3a_{42}a_{43} \\
p_6 &= 30a_{11}a_{12}^2a_{13}^2 + 30a_{21}a_{22}^2a_{23}^2 + 30a_{31}a_{32}^2a_{33}^2 + 30a_{41}a_{42}^2a_{43}^2 \\
p_7 &= a_{13}^5 + a_{23}^5 + a_{33}^5 + a_{43}^5 \\
p_8 &= a_{12}^5 + a_{22}^5 + a_{32}^5 + a_{42}^5 \\
p_9 &= a_{11}^5 + a_{21}^5 + a_{31}^5 + a_{41}^5 \\
p_{10} &= 5a_{11}^4a_{13} + 5a_{21}^4a_{23} + 5a_{31}^4a_{33} + 5a_{41}^4a_{43} \\
p_{11} &= 10a_{11}^3a_{13}^2 + 10a_{21}^3a_{23}^2 + 10a_{31}^3a_{33}^2 + 10a_{41}^3a_{43}^2 \\
p_{12} &= 10a_{11}^2a_{13}^3 + 10a_{21}^2a_{23}^3 + 10a_{31}^2a_{33}^3 + 10a_{41}^2a_{43}^3 \\
p_{13} &= 5a_{11}a_{13}^4 + 5a_{21}a_{23}^4 + 5a_{31}a_{33}^4 + 5a_{41}a_{43}^4 \\
p_{14} &= 5a_{12}^4a_{13} + 5a_{22}^4a_{23} + 5a_{32}^4a_{33} + 5a_{42}^4a_{43} \\
p_{15} &= 10a_{12}^3a_{13}^2 + 10a_{22}^3a_{23}^2 + 10a_{32}^3a_{33}^2 + 10a_{42}^3a_{43}^2 \\
p_{16} &= 10a_{12}^2a_{13}^3 + 10a_{22}^2a_{23}^3 + 10a_{32}^2a_{33}^3 + 10a_{42}^2a_{43}^3 \\
p_{17} &= 5a_{12}a_{13}^4 + 5a_{22}a_{23}^4 + 5a_{32}a_{33}^4 + 5a_{42}a_{43}^4 \\
p_{18} &= 5a_{11}a_{12}^4 + 5a_{21}a_{22}^4 + 5a_{31}a_{32}^4 + 5a_{41}a_{42}^4 \\
p_{19} &= 10a_{11}^2a_{12}^3 + 10a_{21}^2a_{22}^3 + 10a_{31}^2a_{32}^3 + 10a_{41}^2a_{42}^3 \\
p_{20} &= 5a_{11}^4a_{12} + 5a_{21}^4a_{22} + 5a_{31}^4a_{32} + 5a_{41}^4a_{42} \\
p_{21} &= 10a_{11}^3a_{12}^2 + 10a_{21}^3a_{22}^2 + 10a_{31}^3a_{32}^2 + 10a_{41}^3a_{42}^2
\end{aligned}
$$

Using monodromy loops, we find a pseudowitness set of degree 1430. *To test for membership of* T *in* $\sigma_4(\nu_5(\mathbb{P}^2))$, *we use the vector of coefficients corresponding to the monomials in* $x^3y^2 + x^4z$, *which in this case is*

$$(0,0,0,0,0,0,0,0,0,0,1,0,0,0,0,0,0,0,0,0,0,1) \in \mathbb{C}^{21}.$$

We perform the homotopy described above and find $T \in \sigma_4(\nu_5(\mathbb{P}^2))$*, and therefore we conclude* $\operatorname{brk}(T) \leq 4$*.*

Using similar computations, we find a pseudowitness set for $\sigma_3(\nu_5(\mathbb{P}^2))$ *of degree* 859*. Membership testing reveals* $T \notin \sigma_3(\nu_5(\mathbb{P}^2))$ *and therefore we conclude* $\operatorname{brk}(T) = 4$*. This is in agreement with the result of [BB13a].*

Example 5.2.3 *The following example demonstrates that our method computes the* X*-border rank and not a different notion of rank. This example was shown by W. Buczyńska and J. Buczyński as a peculiar but illustrative case where the* X*-border rank of a polynomial cannot be computed by taking limiting points on the Veronese variety [BB13b]. The example is the following:*

$$T = x_0^2 x_2 + 6x_1^2 x_3 - 3(x_0 + x_1)^2 x_4.$$

To test for border rank 5*, we compute a pseudowitness set for* $\sigma_5(\nu_3(\mathbb{P}^4))$*. We find* $\deg \sigma_5(\nu_3(\mathbb{P}^4)) = 24047$*, and a membership test shows* $\operatorname{brk}(T) \leq 5$*. Next, we perform similar computations to test for border rank* 4 *in which we find* $\deg \sigma_4(\nu_3(\mathbb{P}^4)) = 36505$*. The membership test indicates* $\operatorname{brk}(T) > 4$*, and we conclude* $\operatorname{brk}(T) = 5$*. In fact, there exists a sequence of* X*-rank* 5 *elements in* $\mathbb{P}^{19}$ *that converges to* T*, but it is not possible to find a sequence of* 5 *points on* X *whose limit spans a space containing* T *[Ber12], [BB13b].*

5.3 Segre-Grassmann hypersurfaces

In 1770, Waring posed the following question in number theory [War82]: Does each $k \in \mathbb{N}$ have an associated positive integer $s(k)$ such that every natural number is the sum of at most $s(k)$ kth powers of natural numbers? This problem was answered affirmatively by

Hilbert in 1909 [Hil09], but research continues today on variations of Waring's problem. In 2013, Abo and Wan studied a variant of Waring's problem arising in algebraic geometry regarding systems of skew-symmetric forms [AW13]. In their work, Abo and Wan identified several secant varieties of interest that are hypersurfaces. For each hypersurface, both the degree and defining equation were unknown.

We remark that when considering an image of an algebraic set in Chapter 3, we avoided computing defining equations. In Section 3.2.3, we saw that computing polynomials of degree t vanishing on an image in n variables required interpolating at least $\binom{n+t}{n}$ sufficiently general sample points. For small problems, such interpolation may be sufficient to compute the equations defining an image of an algebraic set. For example, in [Som03], the authors use sample points for the twisted cubic curve projected onto a random plane; interpolation is then used to compute equations of the image. Unfortunately, the combinatorial growth in the number of sample points required makes this interpolation impractical in all but the smallest problems.

In the special case of a hypersurface H written as an image of an algebraic set, we may utilize the fact that $H = V(f)$ for a single polynomial $f \in \mathbb{C}[x_1, \ldots, x_n]$ such that

$$\deg H = \deg f.$$

We find that for appropriate problems, determining $\deg f$ by obtaining a pseudowitness set for H is a first step towards computing a symbolic representation of f.

Specifically, we are interested in certain secant varieties of the form

$$\sigma_s(\mathrm{Seg}(\mathbb{P}^m \times \mathbb{G}(k, n)))$$

which are hypersurfaces in certain cases. That is, the objects of interest are $\sigma_s(X)$ where X is the Segre product of a projective m-plane and the Grassmann variety of k-dimensional projective subspaces of an n-dimensional projective space. The Grassmann variety, denoted $\mathbb{G}(k,n)$, is the set of all k-dimensional subspaces of $\mathbb{P}^n$.

Using the algorithm from Section 2.4.2, we are able to compute the degrees of four of these hypersurfaces, which allows us to answer Problem 6.5 from [AW13] and leads to defining polynomials via representation theory. The monodromy approach facilitated by path tracking using `Bertini` yields the following.

Theorem 5.3.1 *The following hold.*

1. *The hypersurface* $\sigma_5(\mathrm{Seg}(\mathbb{P}^2 \times \mathbb{G}(2,5))) \subset \mathbb{P}^{59}$ *has degree 6.*

2. *The hypersurface* $\sigma_5(\mathrm{Seg}(\mathbb{P}^2 \times \mathbb{G}(1,6))) \subset \mathbb{P}^{62}$ *has degree 21.*

3. *The hypersurface* $\sigma_8(\mathrm{Seg}(\mathbb{P}^2 \times \mathbb{G}(1,10))) \subset \mathbb{P}^{164}$ *has degree 33.*

4. *The hypersurface* $\sigma_{11}(\mathrm{Seg}(\mathbb{P}^2 \times \mathbb{G}(1,14))) \subset \mathbb{P}^{314}$ *has degree 45.*

In our execution of the procedure for the hypersurface $\sigma_5(\mathrm{Seg}(\mathbb{P}^2 \times \mathbb{G}(2,5)))$, it took 6 random monodromy loops to compute a pseudowitness set. The last three hypersurfaces are part of an infinite family of hypersurfaces of the form

$$\sigma_{3\ell+2}(\mathrm{Seg}(\mathbb{P}^2 \times \mathbb{G}(1,4\ell+2)))$$

for $\ell \geq 1$. In our execution for these hypersurfaces, it took 13, 12, and 13 random monodromy loops to yield the pseudowitness set for each case, respectively.

All four cases of Theorem 5.3.1 have numerical proofs via the method presented in Section 2.4.2. One may object that the results hold up only to the numerical precision

of our calculations. However, these computations have served as strong evidence and motivation to search for, and eventually find, non-numerical proofs of these results as well as generalizations. These proofs, which utilize representation theory, can be found in [Dal14]. In particular, [Dal14] uses representation theory with the degrees from Theorem 5.3.1 as input to show that these hypersurfaces are minimally defined by known determinantal equations. The defining equation for $\sigma_5(\mathrm{Seg}(\mathbb{P}^2 \times \mathbb{G}(2,5))) \subset \mathbb{P}^{59}$ provides an answer for Problem 6.5 from [AW13]. This degree 6 polynomial in 10080 monomials is presented in an ancillary file to the arXiv version of [Dal14].

5.4 Investigating $\sigma_4(\mathbb{P}^a \times \mathbb{P}^b \times \mathbb{P}^c)$

5.4.1 Statement of the problem

Given vector spaces A, B, C, the *Segre product* is the following embedding into the tensor product:

$$\begin{aligned} \mathrm{Seg} :&\mathbb{P}(A) \times \mathbb{P}(B) \times \mathbb{P}(C) \to \mathbb{P}(A \otimes B \otimes C) \\ &([a],[b],[c]) \mapsto [a \otimes b \otimes c]. \end{aligned}$$

The image of this map is called a *Segre variety*. In this section we study the secant variety $\sigma_k(X)$ where X is a Segre variety as constructed above. Such secant varieties are commonly denoted $\sigma_k(\mathbb{P}^a \times \mathbb{P}^b \times \mathbb{P}^c)$; we omit the mention of Seg when the meaning is clear from context.

The secant variety $\sigma_4(\mathbb{P}^3 \times \mathbb{P}^3 \times \mathbb{P}^3)$ arises in molecular phylogenetics, and in 2007 E. Allman posed the problem of determining its defining ideal [All]. Work on this problem

has led to a set-theoretic solution [Fri13; BO11; FG12], but the ideal-theoretic question is still open. In the following subsections, we use numerical methods to study $\sigma_4(\mathbb{P}^3 \times \mathbb{P}^3 \times \mathbb{P}^3)$ and related secant varieties. The work in this section is adapted from [DH15].

5.4.2 $\sigma_4(\mathbb{P}^3 \times \mathbb{P}^3 \times \mathbb{P}^3)$ and $\sigma_4(\mathbb{P}^2 \times \mathbb{P}^3 \times \mathbb{P}^3)$

The secant variety $\sigma_4(\mathbb{P}^3 \times \mathbb{P}^3 \times \mathbb{P}^3)$ poses a significant computational challenge when we try to work with it directly. When attempting the algorithm of Section 2.4.2 for computing a pseudowitness set, the large degree of $\sigma_4(\mathbb{P}^3 \times \mathbb{P}^3 \times \mathbb{P}^3)$ necessitates tracking of a great number of paths. Consequently, an attempt at performing this algorithm did not terminate.

Given $A' \subset A$, $B' \subset B$, and $C' \subset C$, equations in the ideal of $\sigma_k(\mathbb{P}A' \times \mathbb{P}B' \times \mathbb{P}C')$ can help lead to equations on $\sigma_k(\mathbb{P}A \times \mathbb{P}B \times \mathbb{P}C)$ via a process known as *inheritance* [LM04]. This motivates us to consider secant varieties related to $\sigma_4(\mathbb{P}^3 \times \mathbb{P}^3 \times \mathbb{P}^3)$ rather than working with it directly. For example, when we consider $\sigma_4(\mathbb{P}^2 \times \mathbb{P}^3 \times \mathbb{P}^3)$, we are able to compute a pseudowitness set and find the following result.

Proposition 5.4.1 *The secant variety* $\sigma_4(\mathbb{P}^2 \times \mathbb{P}^3 \times \mathbb{P}^3)$ *has degree* 252776.

In addition to providing the degree of $\sigma_4(\mathbb{P}^2 \times \mathbb{P}^3 \times \mathbb{P}^3)$, this pseudowitness set can be used to test points for membership as described in Section 5.2.

A theorem of Landsberg and Manivel [LM08] with an error in the proof corrected by Friedland [Fri13] shows how $\sigma_4(\mathbb{P}^2 \times \mathbb{P}^2 \times \mathbb{P}^3)$ can be used to inform us about $\sigma_4(\mathbb{P}^a \times \mathbb{P}^b \times \mathbb{P}^c)$ for any $a, b, c \geq 3$. Thus, we turn our attention to $\sigma_4(\mathbb{P}^2 \times \mathbb{P}^2 \times \mathbb{P}^3)$.

5.4.3 $\sigma_4(\mathbb{P}^2 \times \mathbb{P}^2 \times \mathbb{P}^3)$

Let $S = \sigma_4(\mathbb{P}^2 \times \mathbb{P}^2 \times \mathbb{P}^3) \subset \mathbb{P}^{35}$. In [BO11], numerical computations showed that S is set-theoretically defined by 10 polynomials of degree 6 and 20 polynomials of degree 9. This result, which was used to determine set-theoretic defining equations for $\sigma_4(\mathbb{P}^3 \times \mathbb{P}^3 \times \mathbb{P}^3)$, was also shown without the use of a computer in [FG12]. Here, we apply the methods of Chapter 3 to show that S is aCM and use this to show that $I(S)$ is minimally generated by 10 polynomials of degree 6 and 20 polynomials of degree 9.

Rather than start with known polynomials vanishing on S, we derive our results from a parameterization of S. In particular, consider the map $\pi : \mathbb{C}^{12} \times \mathbb{C}^{12} \times \mathbb{C}^{16} \to \mathbb{C}^{36}$ defined by

$$(\mathbf{a}, \mathbf{b}, \mathbf{c}) \mapsto \sum_{\ell=1}^{4} a_{i\ell} b_{j\ell} c_{k\ell} \text{ for } 1 \leq i, j \leq 3 \text{ and } 1 \leq k \leq 4.$$

If $Y = \overline{\pi(\mathbb{C}^{12} \times \mathbb{C}^{12} \times \mathbb{C}^{16})} \subset \mathbb{C}^{36}$, then S is the projectivization of Y, namely $S = \mathbb{P}(Y) \subset \mathbb{P}^{35}$. Using π, we verify that S is non-defective with $\dim S = 31$. After selecting a random linear space $\mathcal{L} \subset \mathbb{P}^{35}$ of codimension 30 and random hyperplane $\mathcal{H} \subset \mathbb{P}^{35}$, consider the curve $C = X \cap \mathcal{L}$ and witness point set $W = C \cap \mathcal{H}$. We used `Bertini` to compute W and the strategy described in Section 2.4.2 to compute a pseudowitness set for $C = S \cap \mathcal{L}$. This computation, in particular, verified that $\deg S = 345$ as reported in [BO11]. Interpolation and [Gri14] produces

$$HF_W = 1, 5, 15, 35, 70, 126, 200, 280, 345, 345$$

$$HF_C = 1, 6, 21, 56, 126, 252, 452, 732, 1077, 1422$$

$$\Delta HF_C = 1, 5, 15, 35, 70, 126, 200, 280, 345, 345$$

which, by Corollary 3.3.3 and Theorem 3.4.1, shows that both C and S are aCM. Since $\rho_W = 8$, we know $\operatorname{reg} S = \operatorname{reg} C = \operatorname{reg} W = 9$, $\rho_C = 7$, and $\rho_S = -23$. In particular, (3.8) yields $g_C = 1684$ and the strategy outlined in Section 3.4 provides

$$\begin{aligned} HF_S &= 1, 36, 666, 8436, 82251, 658008, 4496378, 26977968, 145001853, 708846128, \ldots \\ HS_S(t) &= (1 + 4t + 10t^2 + 20t^3 + 35t^4 + 56t^5 + 74t^6 + 80t^7 + 65t^8)/(1-t)^{32} \\ HP_S(t) &= 345/31! \cdot t^{31} + \cdots + 299405047890287/72201776446800 \cdot t + 1. \end{aligned}$$

In fact, $\rho_S = -23$ so that $HP_S(j) = 0$ for $-23 \leq j \leq -1$, and $HP_S(t)$ can be written as

$$\begin{aligned} HP_S(t) &= \frac{G(t)}{31!} \prod_{j=1}^{23} (t+j) \quad \text{where} \\ G(t) &= 345 \cdot t^8 + 13032 \cdot t^7 + 484578 \cdot t^6 + 11904840 \cdot t^5 + 218110185 \cdot t^4 \\ &\quad + 2831500368 \cdot t^3 + 24772341372 \cdot t^2 + 131202341280 \cdot t + 318073392000. \end{aligned}$$

We now turn our attention to describing a minimal generating set for $I(S)$ using Prop. 3.4.4. Since $\operatorname{reg} S = 9$, we know that $I(S)$ is minimally generated by polynomials of degree at most 9. That is, $d_j(W) = d_j(S) = 0$ for $j \geq 10$. Moreover, $d_j(W) = d_j(S) = 0$ for $0 \leq j \leq 5$, since $HF_W(t) = \binom{4+t}{t}$ for $0 \leq t \leq 5$. Also, $HF_W(6) = \binom{4+6}{6} - 10$ yields $d_6(W) = d_6(X) = 10$ with the initial degree of X being 6. Using linear algebra, we verified that this 10 dimensional space of sextic polynomials vanishing on W generates a 50 dimensional space of septic polynomials, a 150 dimensional space of octic polynomials, and a 350 dimensional space of nonic polynomials. Since $HF_W(7) = \binom{4+7}{7} - 50$, $HF_W(8) = \binom{4+8}{8} - 150$, and $HF_W(9) = \binom{4+9}{9} - 370$, we know $d_W(7) = d_S(7) = d_W(8) = d_S(8) = 0$ and $d_W(9) = d_S(9) = 20$. Therefore, $I(S)$ is minimally generated by 10 sextic polynomials

and 20 nonic polynomials.

Up to high numerical accuracy, our results suggest that the set-theoretic solution found in [BO11; FG12] is in fact an ideal-theoretic solution to Allman's problem.

REFERENCES

[AW13] Abo, H. & Wan, J. "On Waring's problem for systems of skew-symmetric forms". *Linear Algebra Appl.* **439**.8 (2013), pp. 2330–2349.

[Ace05] Acebrón, J. et al. "The Kuramoto model: A simple paradigm for synchronization phenomena". *Reviews of modern physics* **77**.1 (2005), p. 137.

[AR04] Aeyels, D. & Rogge, J. A. "Existence of partial entrainment and stability of phase locking behavior of coupled oscillators". *Progress on Theoretical Physics* **112**.6 (2004), pp. 921–942.

[All] Allman, E. *Open problem: Determine the ideal defining* $\mathrm{Sec}^4(\mathbb{P}^3 \times \mathbb{P}^3 \times \mathbb{P}^3)$. Available at `www.dms.uaf.edu/~eallman/Papers/salmonPrize.pdf`.

[AR08] Allman, E. S. & Rhodes, J. A. "Phylogenetic ideals and varieties for the general Markov model". *Advances in Applied Mathematics* **40**.2 (2008), pp. 127–148.

[Amr96] Amrhein, B. et al. "A case study of multi-threaded Gröbner basis completion". *Proceedings of the 1996 international symposium on Symbolic and algebraic computation*. ACM. 1996, pp. 95–102.

[Ara81] Araposthatis, A. et al. "Analysis of power-flow equation". *International Journal of Electrical Power & Energy Systems* **3**.3 (1981), pp. 115–126.

[BB82] Baillieul, J. & Byrnes, C. I. "Geometric critical point analysis of lossless power system models". *IEEE Transactions on Circuits and Systems* **29**.11 (1982), pp. 724–737.

[BB13a] Ballico, E. & Bernardi, A. "Stratification of the fourth secant variety of Veronese varieties via the symmetric rank". *Advances in Pure and Applied Mathematics* **4**.2 (2013), pp. 215–250.

[BO11] Bates, D. & Oeding, L. "Toward a salmon conjecture". *Exp. Math.* **20**.3 (2011), pp. 358–370.

[Bat] Bates, D. et al. *Bertini: Software for numerical algebraic geometry (versions 1.3–1.5)*. Available at `bertini.nd.edu`.

[Bat11] Bates, D. et al. "Numerical computation of the genus of an irreducible curve within an algebraic set". *J. Pure Appl. Algebra* **215**.8 (2011), pp. 1844–1851.

[Bat13] Bates, D. et al. *Numerically solving polynomial systems with Bertini*. Vol. 25. SIAM, 2013.

[BS87] Bayer, D. & Stillman, M. "A criterion for detecting m-regularity". *Invent. Math.* **87**.1 (1987), pp. 1–11.

[Ber15] Bernardi, A. et al. "Tensor decomposition and homotopy continuation". *In preparation* (2015).

[Ber12] Bernardi, A. et al. "A comparison of different notions of ranks of symmetric tensors" (2012). arXiv: 1210.8169.

[Boi11] Boij, M. et al. "Monomials as sums of powers: the real binary case". *Proceedings of the American Mathematical Society* **139**.9 (2011), pp. 3039–3043.

[Buc65] Buchberger, B. "An algorithmic criterion for the solvability of algebraic systems of equations". PhD thesis. University of Innsbruck, 1965.

[BB13b] Buczyńska, W. & Buczyński, J. "On differences between the border rank and the smoothable rank of a polynomial" (2013). arXiv: 1305.1726.

[Car12] Carlini, E. et al. "The solution to the Waring problem for monomials and the sum of coprime monomials". *Journal of Algebra* **370** (2012), pp. 5–14.

[Casne] Casetti, L. et al. "Phase Transitions and Topology Changes in Configuration Space". *Journal of Statistical Physics* **111** (June 2003), 1091–1123(33).

[Che05] Chevalier, P. et al. "On the virtual array concept for higher order array processing". *Signal Processing, IEEE Transactions on* **53**.4 (2005), pp. 1254–1271.

[Cio09] Cioffi, F. et al. "Regularity bounds by minimal generators and Hilbert function". *Collect. Math.* **60**.1 (2009), pp. 89–100.

[Com92] Comon, P. "Independent component analysis". *Higher-Order Statistics* (1992), pp. 29–38.

[Com02] Comon, P. "Tensor decompositions, state of the art and applications". *Mathematics in Signal Processing V* (2002), pp. 1–24.

[CJ10] Comon, P. & Jutten, C. *Handbook of Blind Source Separation: Independent component analysis and applications*. Academic press, 2010.

[Cox07] Cox, D. et al. *Ideals, varieties, and algorithms*. Third. Undergraduate Texts in Mathematics. An introduction to computational algebraic geometry and commutative algebra. Springer, New York, NY, 2007, pp. xvi+551.

[DH15] Daleo, N. & Hauenstein, J. "Numerically deciding the arithmetically Cohen-Macaulayness of a projective scheme". *Journal of Symbolic Computation* **In press** (2015). DOI: 10.1016/j.jsc.2015.01.001.

[Dal14] Daleo, N. et al. "Computations and equations for Segre-Grassmann hypersurfaces" (2014). arXiv: 1408.2105.

[DLC07] De Lathauwer, L. & Castaing, J. "Tensor-based techniques for the blind separation of DS-CDMA signals". *Signal Processing* **87**.2 (2007), pp. 322–336.

[DB14] Dörfler, F. & Bullo, F. "Synchronization in Complex Oscillator Networks: A survey". *Automatica* **50**.6 (2014), pp. 1539–1564.

[Dör13] Dörfler, F. et al. "Synchronization in Complex Oscillator Networks and Smart Grids". *Proceedings of the National Academy of Sciences* **110**.6 (2013), pp. 2005–2010.

[DB11] Dörfler, F. & Bullo, F. "On the critical coupling for Kuramoto oscillators". *SIAM Journal on Applied Dynamical Systems* **10**.3 (2011), pp. 1070–1099.

[EF14] Eder, C. & Faugère, J.-C. "A survey on signature-based Gröbner basis computations" (2014). arXiv: 1404.1774.

[EG05] Eisert, J. & Gross, D. "Multi-particle entanglement" (2005). arXiv: quant-ph/0505149.

[Erm85] Ermentrout, G. B. "The behavior of rings of coupled oscillators". *Journal of mathematical biology* **23**.1 (1985), pp. 55–74.

[Fau99] Faugère, J.-C. "A new efficient algorithm for computing Gröbner bases (F4)". *Journal of pure and applied algebra* **139**.1 (1999), pp. 61–88.

[Fau02] Faugère, J.-C. "A new efficient algorithm for computing Gröbner bases without reduction to zero (F5)". *Proceedings of the 2002 International Symposium on Symbolic and Algebraic Computation*. ISSAC '02. New York, NY, USA: ACM, 2002, pp. 75–83.

[FG12] Friedland, S. & Gross, E. "A proof of the set-theoretic version of the salmon conjecture". *J. Algebra* **356** (2012), pp. 374–379.

[Fri13] Friedland, S. "On tensors of border rank l in $C^{m\times n\times l}$". *Linear Algebra and its Applications* **438**.2 (2013), pp. 713–737.

[Gor99] Gordon, P. "Neuer Beweis des Hilbertschen Satzes über homogene Funktionen". *Nachrichten König. Ges. der Wiss. zu Gött* (1899), pp. 240–242.

[Gor06] Gorla, E. "The general hyperplane section of a curve". *Trans. Am. Math. Soc.* **358**.2 (2006), pp. 819–869.

[Gra06] Gray, J. et al. "Exploring the vacuum geometry of $\mathcal{N} = 1$ gauge theories". *Nucl. Phys. B* **750**.1 (2006), pp. 1–27.

[GS] Grayson, D. & Stillman, M. *Macaulay2, a software system for research in algebraic geometry*. Available at `www.math.uiuc.edu/Macaulay2`.

[Gri14] Griffin, Z. et al. "Numerical computation of the Hilbert function of a zero-scheme". *Springer Proc. Math. Stat.* **76** (2014), pp. 235–250.

[Gru83] Gruson, L. et al. "On a theorem of Castelnuovo, and the equations defining space curves". *Invent. Math.* **72**.3 (1983), pp. 491–506.

[Has06] Hassett, B. "Introduction to algebraic geometry". *AMC* **10** (2006).

[HS10] Hauenstein, J. & Sommese, A. "Witness sets of projections". *Appl. Math. Comput.* **217**.7 (2010), pp. 3349–3354.

[HS13] Hauenstein, J. & Sommese, A. "Membership tests for images of algebraic sets by linear projections". *Appl. Math. Comput.* **219**.12 (2013), pp. 6809–6818.

[HW13] Hauenstein, J. & Wampler, C. "Isosingular sets and deflation". *Found. Comp. Math.* **13**.3 (2013), pp. 371–403.

[Hau09] Hauenstein, J. et al. "Numerical computation of the dimensions of the cohomology of twists of ideal sheaves". *Contemp. Math.* **496** (2009), pp. 235–242.

[Hau13a] Hauenstein, J. et al. "Equations for lower bounds on border rank". *Experimental Mathematics* **22**.4 (2013), pp. 372–383.

[Hau13b] Hauenstein, J. et al. "Numerical elimination and moduli space of vacua". *J. High Energy Phys.* **2013**.9 (2013), pp. 1–28.

[Hau14] Hauenstein, J. D. et al. "Homotopy techniques for tensor decomposition and perfect identifiability" (2014). arXiv: 1501.00090.

[Hil09] Hilbert, D. "Beweis für die Darstellbarkeit der ganzen Zahlen durch eine feste Anzahl n^{ter} Potenzen (Waringsches Problem)". *Mathematische Annalen* **67** (1909), pp. 281–300.

[Hug13] Hughes, C. et al. "Enumerating Gribov copies on the lattice". *Annals Phys.* **331** (2013), pp. 188–215. arXiv: 1203.4847 [hep-lat].

[HU93] Huneke, C. & Ulrich, B. "General hyperplane sections of algebraic varieties". *J. Algebraic Geom* **2**.3 (1993), pp. 487–505.

[JS04] Jiang, T. & Sidiropoulos, N. "Kruskal's permutation lemma and the identification of CANDECOMP/PARAFAC and bilinear models with constant modulus constraints". *Signal Processing, IEEE Transactions on* **52**.9 (2004), pp. 2625–2636.

[Kas11] Kastner, M. "Stationary-point approach to the phase transition of the classical XY chain with power-law interactions". *Physical Review E* **83**.3 (2011), p. 031114.

[Kon04] Kondratyev, A. et al. "Numerical computation of Gröbner bases". *Proceedings of CASC2004 (Computer Algebra in Scientific Computing)* (2004), pp. 295–306.

[Kro13] Krone, R. "Numerical algorithms for dual bases of positive-dimensional ideals". *J. Algebra. Appl.* **12**.06 (2013), p. 1350018.

[Kur75] Kuramoto, Y. "Self-entrainment of a population of coupled non-linear oscillators". *International symposium on mathematical problems in theoretical physics*. Springer. 1975, pp. 420–422.

[LM04] Landsberg, J. M. & Manivel, L. "On the ideals of secant varieties of Segre varieties". *Foundations of Computational Mathematics* **4**.4 (2004), pp. 397–422.

[LM08] Landsberg, J. M. & Manivel, L. "Generalizations of Strassen's equations for secant varieties of Segre varieties". *Communications in Algebra* **36**.2 (2008), pp. 405–422.

[Mac02] Macaulay, F. "Some formulae in elimination". *Proc. London Math. Soc.* **35** (1902).

[Map12] Maplesoft. *Maple 16*. Waterloo, Ontario, 2012.

[Mat14] MathWorks. *MATLAB R2014b*. Natick, Massachusetts, 2014.

[McC87] McCullagh, P. *Tensor methods in statistics*. Vol. 161. Chapman and Hall London, 1987.

[Meh09a] Mehta, D. "Lattice vs. Continuum: Landau Gauge Fixing and t́ Hooft-Polyakov Monopoles". PhD thesis. University of Adelaide, 2009.

[Meh14] Mehta, D. et al. "Gauge-fixing on the lattice via orbifolding". *Phys. Rev. D* **90** (2014), p. 054504.

[Meh15] Mehta, D. et al. "Algebraic geometrization of the Kuramoto model: Equilibria and stability analysis". *Chaos: An Interdisciplinary Journal of Nonlinear Science* **To appear** (2015).

[MK11] Mehta, D. & Kastner, M. "Stationary point analysis of the one-dimensional lattice Landau gauge fixing functional, aka random phase XY Hamiltonian". *Annals Phys.* **326** (2011), pp. 1425–1440. arXiv: `1010.5335 [cond-mat.stat-mech]`.

[MS14] Mehta, D. & Schröck, M. "Enumerating Copies in the First Gribov Region on the Lattice in up to four Dimensions" (2014). arXiv: `1403.0555 [hep-lat]`.

[Meh09b] Mehta, D. et al. "Lattice Landau Gauge and Algebraic Geometry". *PoS* **QCD-TNT09** (2009), p. 025. arXiv: `0912.0450 [hep-lat]`.

[Mig98] Migliore, J. *Introduction to Liaison Theory and Deficiency Modules*. Vol. 165. Birkhäuser Boston, Boston, MA, 1998.

[MS05] Mirollo, R. E. & Strogatz, S. H. "The spectrum of the locked state for the Kuramoto model of coupled oscillators". *Physica D: Nonlinear Phenomena* **205**.1-4 (2005), pp. 249–266.

[Ner13] Nerattini, R. et al. "Exploring the energy landscape of XY models". *Phys.Rev.* **E87**.3 (2013), p. 032140. arXiv: `1211.4800 [cond-mat.stat-mech]`.

[OG09] Ochab, J & Góra, P. "Synchronization of coupled oscillators in a local one-dimensional Kuramoto model" (2009). arXiv: `0909.0043`.

[RS11] Ranestad, K. & Schreyer, F.-O. "On the rank of a symmetric form". *Journal of Algebra* **346**.1 (2011), pp. 340–342.

[Ros14] Rosen, Z. "Computing algebraic matroids" (2014). arXiv: 1210.8169.

[SS08] Schultz, T. & Seidel, H.-P. "Estimating crossing fibers: A tensor decomposition approach". *Visualization and Computer Graphics, IEEE Transactions on* **14**.6 (2008), pp. 1635–1642.

[Sid00] Sidiropoulos, N. D. et al. "Blind PARAFAC receivers for DS-CDMA systems". *Signal Processing, IEEE Transactions on* **48**.3 (2000), pp. 810–823.

[Sme07] Smekal, L. von et al. "Modified Lattice Landau Gauge". *PoS* **LAT2007** (2007), p. 382.

[Sme08] Smekal, L. von et al. "Lattice Landau gauge via Stereographic Projection". *PoS* **CONFINEMENT8** (2008), p. 048.

[Smi05] Smilde, A. et al. *Multi-way analysis: applications in the chemical sciences*. John Wiley & Sons, 2005.

[SW05] Sommese, A. & Wampler, C. *The Numerical Solution of Systems of Polynomials Arising in Engineering and Science*. World Scientific Publishing, Hackensack, NJ, 2005.

[Som96] Sommese, A. et al. "Numerical algebraic geometry". *The Mathematics of Numerical Analysis, volume 32 of Lectures in Applied Mathematics*. Citeseer. 1996.

[Som01] Sommese, A. et al. "Numerical decomposition of the solution sets of polynomial systems into irreducible components". *SIAM Journal on Numerical Analysis* **38**.6 (2001), pp. 2022–2046.

[Som03] Sommese, A. J. et al. "Numerical irreducible decomposition using PHCpack". *Algebra, Geometry and Software Systems*. Springer, 2003, pp. 109–129.

[Str83] Strassen, V. "Rank and optimal computation of generic tensors". *Linear algebra and its applications* **52** (1983), pp. 645–685.

[SM88] Strogatz, S. H. & Mirollo, R. E. "Phase-locking and critical phenomena in lattices of coupled nonlinear oscillators with random intrinsic frequencies". *Physica D: Nonlinear Phenomena* **31**.2 (1988), pp. 143–168.

[Str00] Strogatz, S. “From Kuramoto to Crawford: exploring the onset of synchronization in populations of coupled oscillators”. *Physica D: Nonlinear Phenomena* **143**.1 (2000), pp. 1–20.

[Tay12] Taylor, R. “There is no non-zero stable fixed point for dense networks in the homogeneous Kuramoto model”. *Journal of Physics A: Mathematical and Theoretical* **45**.5 (2012), p. 055102.

[Val01] Valiant, L. G. “Quantum computers that can be simulated classically in polynomial time”. *Proceedings of the thirty-third annual ACM symposium on Theory of computing*. ACM. 2001, pp. 114–123.

[VM08] Verwoerd, M. & Mason, O. “Global phase-locking in finite populations of phase-coupled oscillators”. *SIAM Journal on Applied Dynamical Systems* **7**.1 (2008), pp. 134–160.

[VM09] Verwoerd, M. & Mason, O. “On computing the critical coupling coefficient for the Kuramoto model on a complete bipartite graph”. *SIAM Journal on Applied Dynamical Systems* **8**.1 (2009), pp. 417–453.

[War82] Waring, E. *Meditationes algebricae, ed. III*. Cambridge, 1782.

[Wil06] Wiley, D. A. et al. “The size of the sync basin”. *Chaos: An Interdisciplinary Journal of Nonlinear Science* **16**.1 (2006), p. 015103.